

Magnesium-Based Hydrogen Storage Compounds: A Review

Liuzhang Ouyang,^{a, b *} Fen Liu,^a Hui Wang,^a Jiangwen Liu^a, Xu-Sheng Yang,^{c, d *}

Lixian Sun,^{e *} and Min Zhu^a

^a School of Materials Science and Engineering and Key Laboratory of Advanced Energy Storage Materials of Guangdong Province, South China University of Technology, Guangzhou, 510641, China

^b China-Australia Joint Laboratory for Energy & Environmental Materials, Key Laboratory of Fuel Cell Technology of Guangdong Province, Guangzhou, Guangzhou, 510641, China

^c Advanced Manufacturing Technology Research Centre, Department of Industrial and Systems Engineering, The Hong Kong Polytechnic University, Hung Hom, Kowloon, Hong Kong

^d Hong Kong Polytechnic University Shenzhen Research Institute, Shenzhen 518057, China

^e Guangxi Key Laboratory of Information Materials, Guangxi Collaborative Innovation Center of Structure and Property for New Energy, Materials and School of Materials Science and Engineering, Guilin University of Electronic Technology, Guilin, 541004, China

* Corresponding Author:

Liuzhang Ouyang: E-mail: meouyang@scut.edu.cn; Tel: +86 20 87111317

Xu-Sheng Yang: E-mail: xsyang@polyu.edu.hk; Tel: +852-27666604

Lixian Sun: E-mail: sunlx@guet.edu.cn)

Abstract: One of the key points to boost the application of fuel cells is the progress in the development of hydrogen storage alloys with appealing high capacity. Of the numerous candidate alloys for storing hydrogen, magnesium (Mg)-based alloys have been progressively attracting great attention owing to their abundance, low densities, and considerable capacities of hydrogen storage. Nevertheless, the practical applications of Mg-based hydrogen storage alloys are still seriously hampered by their sluggish kinetics and relative stable thermodynamic characteristics. At present, some strategies have been utilizing to tune the hydrogen storage properties of Mg-based alloys, but they are still insufficient to fulfill the requirements for practical industrial applications. In this review, advanced synthetic approaches and some effective strategies including alloying, nanostructuring, doping by catalytic additives and forming nanocomposites with other hydrides, etc., to enhance the requirements properties of Mg-based hydrogen storage alloys are summarized, and then the prospects for further promoting the properties of Mg-based hydrogen storage materials are also briefly discussed.

Keywords: Metal hydride; Mg-based hydrogen storage alloys; thermodynamics; alloying; nanostructuring; forming nanocomposites

1. Introduction

Future energy requests urgently desire substitutes for the present energy technologies that are relied chiefly on fossil fuels.[1] Hydrogen is a promising and broadly expected selection as an alternative energy feedstock.[2-4] The primary technical components of the hydrogen energy system cover the production, supply, storage, conversion, and employment of hydrogen, among which the storage and conversion of hydrogen are consistently the keys to the effective utilization of hydrogen energy. The conventional hydrogen storage approach mostly uses cylinders to store hydrogen, which has the drawbacks of inferior efficiency, excessive pressure hindrance, and leakage prevention. Owing to their high storage densities by human concern, hydrogen storage materials have been developed into one of the crucial functional materials in materials science exploration. Hydrogen storage material, as an extraordinarily significant applied material, plays a unique part in the field of secondary energy, exceptionally in the area of fuel cells and secondary batteries. Additionally, researches regarding the hydrogen storage material can be not only directly united with the application of electric vehicles, but also with the submarine, spacecraft and other fields with considerable impacts.[5] In recent several decades, enormous endeavors have been carried out to push the hydrogen storage alloys to achieve the desire for fairly competent solid-state hydrogen storage, which will be indispensable for the prospective hydrogen economy.

The current metallic hydrogen storage materials^{3,19} can be generally divided into several categories, such as rare earth systems (e.g., LaNi_5), titanium- (e.g., FeTi), zirconium- (e.g., ZrMn), and magnesium (Mg) -based alloys (e.g., Mg_2Ni), etc. The hydrogen density of some representative hydrogen storage alloys is summarized in Figure 1.[6] Of the primary hydrogen storage alloys progressed formerly, Mg and Mg-

based hydrogen storage materials are believed to provide the remarkable possibility of the practical application, on account of the advantages as following: 1) the resource of Mg is plentiful and economical. Mg element exists abundantly and accounts for ~2.35 % of the earth's crust with the rank of the eighth; 2) low density of merely $1.74 \text{ g}\cdot\text{cm}^{-3}$; 3) superior hydrogen storage capacity. The theoretical hydrogen storage amounts of the pure Mg is 7.6 wt. % (weight percent), [7-9] and the Mg_2Ni is 3.6 wt.%, respectively.

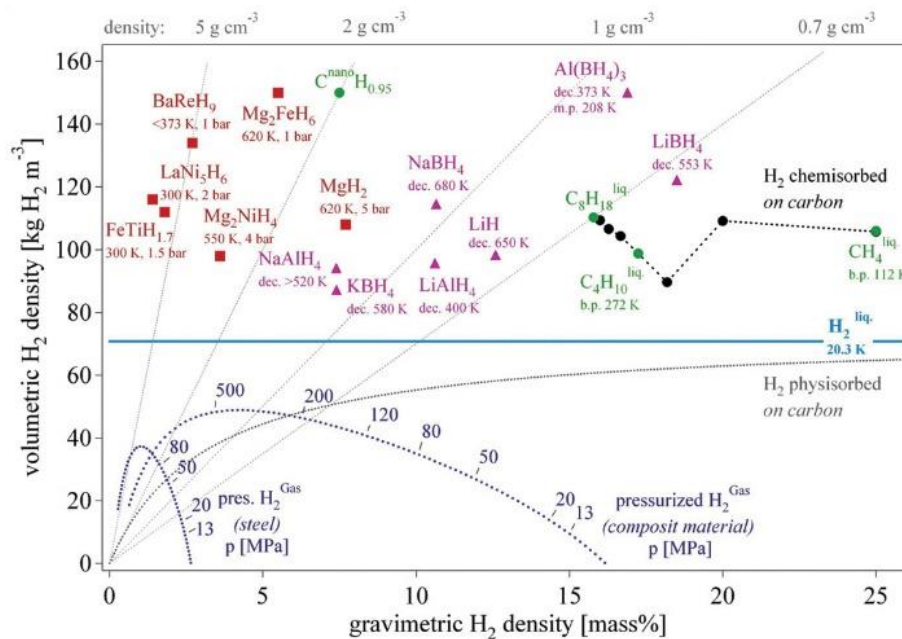


Fig. 1. Gravimetric and volumetric hydrogen density of some representative metallic hydrogen storage materials. Reproduced by permission from Züttel *et al.*, Mater. Today 6, 24 (2003). Mater. Today 6, 24 (2003). Copyright 2003 by Elsevier.

Mg-based hydrogen storage materials can be generally fell into three categories, i.e., pure Mg, Mg-based alloys, and Mg-based composites. Particularly, more than 300 sorts of Mg-based hydrogen storage alloys have been receiving extensive attention, [10] because of the relatively better overall performance. Nonetheless, the inferior hydrogen absorption/desorption kinetics rooting in the overly undue thermodynamic stability of

metal hydride make the Mg-based hydrogen storage alloys currently not appropriate for the real applications, and therefore, massive attempts have been dedicated to overcoming these shortages. Some sample preparation methods, such as smelting, powder sintering, diffusion, mechanical alloying, hydriding combustion synthesis method, surface treatment, and heat treatment, etc., have been broadly employed for altering the dynamic performance and cycle life of Mg-based hydrogen storage alloys. Besides, some intrinsic modification strategies, including alloying,[11-14] nanostructuring,[15-20] doping by catalytic additives,[21] and acquiring nanocomposites with other hydrides,[22-29] etc., have been mainly explored for intrinsically boosting the performance of Mg-based hydrogen storage alloys. Albeit considerable breakthrough has been attained, further endeavors are desired to enhance the properties of these materials.

In this review paper, after briefly introducing the basic information of Mg-based hydrogen storage alloys in this Section 1. Then, the classification of Mg-based hydrogen storage alloys will be summarized in Section 2; the main approaches to modifying the properties of Mg-based alloys will be discussed in Section 3 and finally the conclusive statements, observations, and the research prospects of the Mg-based hydrogen storage materials will be provided in Section 4.

2. Mg-based alloys classification

Though the hydrogen storage capacity of pure Mg is comparatively outstanding, the discontentedly high desorption hydrogen temperature and sluggish kinetics gravely block its practical applications.[2, 7, 21, 30-33] Diverse metals, counting rare earth (RE) (e.g. Ce, La), non-transition (e.g. Al, Li, In) and transition metals (e.g. Ni, Co, Fe, Cu, Ag, Sc, Y), etc., have been adopted to form Mg-based alloys for years, in which the relatively less stable hydride MgH_2 can be alloyed with Mg, so as to undermine the

thermodynamic stability of its hydride. The strategy, comparable to that applied to AB₅ (such as LaNi₅), AB₂ (such as ZrMn₂), and AB (such as FeTi) hydrides, where the A element has a larger affinity for hydrogen than the B element, has been found to be the appropriate alloying mix of Mg and a non-stable hydride to adequately reduce the strength of Mg-H bond. Three categorizations of Mg-based alloys, i.e., intermetallic compounds, solid-solution compounds and other compounds, are discussed in the following three sub-sections.

2.1 Intermetallic compounds

The hydrogen storage material for realizing hydrogen as a fuel in mobile appliances has to meet stringent requirements, such as the hydrogen capacity, the stability of hydride, the hydrogen exchange rates, economy, and safety. In particular, the reversibility of the reactions between hydrogen and metals, alloys or intermetallic compounds would also highly affect their practical applications. As for the Mg-based hydrogen storage intermetallic compounds, some of them can reversibly absorb hydrogen and the original starting material can be regenerated. However, the reaction pathway of some other Mg-based hydrogen storage intermetallic compounds with hydrogen is usually irreversible and often complex. Therefore, the Mg-based hydrogen storage intermetallic compounds are summarized into three categories in this section, according to their hydrogenation/dehydrogenation routes.

2.1.1 Reversible Mg-based hydrogen storage alloys

Two representative reversible Mg-based hydrogen storage intermetallic compounds, which can absorb hydrogen and release hydrogen reversibly, are Mg-Ni alloys and Mg-Fe alloys. In this section, we will mainly introduce these two types of alloys and focus on the effects of the addition of the other elements on the enhancement of their

hydrogen storage properties, including thermodynamic and kinetic properties.

(1) Mg-Ni alloys

An acclaimed of representative Mg-based compounds is Mg_2Ni , which generates Mg_2NiH_4 hydride during hydrogenation. It owns a low enthalpy of hydrogen desorption ($\Delta H = 64.5 \text{ kJ (mol}^{-1} \text{ H}_2\text{)}$). The Mg-based hydrogen storage materials were first investigated at Brookhaven National Laboratory, where Reilly and Wiswall prepared Mg_2Ni in an induction furnace under argon and introduced the reaction of hydrogen with Mg-Ni alloys at elevated temperatures and pressures.[34] It turned out that Mg_2Ni alloy can react readily with hydrogen, forming Mg_2NiH_4 at 300°C under 2 MPa, with a storage capacity of 3.6 wt.%. Besides, the specific study of the hydrogen storage properties and mechanisms of Mg_2Ni found that: 1) The pressure-compositional temperature (PCT) curve of Mg_2Ni alloy was flat with a small lag, as shown in Figure 2; 2) Ni played a key catalytic role in making Mg easier to absorb and release hydrogen. Nonetheless, the hydrogen release temperature and powder resistance stability of Mg_2Ni alloy is still needed to be further improved.

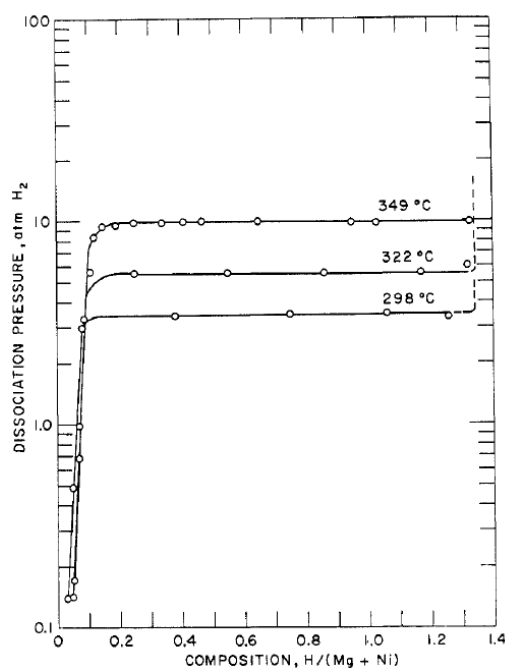


Fig. 2. Desorption isotherms for the $\text{Mg}_2\text{Ni-H}$ system. The initial alloy composition is 45.9 wt.% Mg and 54.6 wt.% Ni. Reproduced by permission from Reilly *et al.*, Inorg. Chem. 7, 2254 (1968). Copyright 1968 by ACS publications.

The addition of the third element, namely M, to Mg_2Ni has been extensively employed to enhance the hydrogen storage properties of Mg_2Ni , either further reduce the temperature or boost the kinetic properties of hydrogen absorption and release processes. The added M elements include copper (Cu), zinc (Zn), palladium (Pd), chromium (Cr), manganese (Mn), cobalt (Co), Ni, Mg, zirconium (Zr), vanadium (V) and RE elements, etc.[35] In general, the M component in the $\text{Mg}_2\text{Ni-M}$ alloy takes up a relatively small proportion, normally less than 15 wt.%, and it can partially replace Ni or Mg. For example, amorphous and nanocrystalline Mg-Ni-RE alloys (RE = Y, Ce, La, Mm) formed by prompt solidification have seized the attention of researchers considering the improved hydrogenation characteristics.[36-39] However, it was reported that the maximum hydrogen storage capacity of the amorphous or nanocrystalline Mg-Ni-RE alloys was less than 5 wt.%, derived from the great number of Ni and RE and the comparatively large grain size of 100-150 nm. Accordingly, it is raring to redesign the composition together with the production approach of alloys. Yao and his colleagues[40, 41] raised Mg-based nanocomposites, possessing 4.7 nm grain size on average, and fine-grained Mg_2Ni nanoparticles holding the size of ~ 2.7 nm via mechanical milling the amorphous Mg-10Ni-5Y along with the advanced nanocarbon supported metallic catalyst. As a result, this nanocomposite system exhibits ultrafast hydrogenation kinetics and acquires a summit hydrogen storage capacity of 6 wt.%.

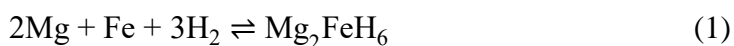
To dual tune the thermodynamic and kinetic properties of Mg_2Ni , Ouyang *et al.*[42] prepared $\text{Mg}_2\text{NiIn}_{0.1}$ solid solution via two steps, particularly sintering of the elemental powders and ball milling in succession. Introducing In into Mg_2Ni can considerably

improve its dehydrogenation kinetics as well as markedly diminish its thermodynamic stability, by which the dehydrogenation activation energy (E_a) and enthalpy change (ΔH) decreases from 80 kJ mol⁻¹ and 64.5 kJ (mol⁻¹ H₂) to 28.9 kJ mol⁻¹ and 38.4 kJ (mol⁻¹ H₂), respectively. The attained consequences indicate a way to tune thermodynamic along with kinetic properties of hydrogen storage materials.

In addition to Mg₂Ni alloy, Mg can form another type of intermetallic compound with Ni, viz. MgNi₂, which barely reacts with hydrogen despite heating to 623 K in its regular polycrystalline phase status.[34, 43] However, nanostructured MgNi₂ formed via ball milling has been proved to be able to interact easily with hydrogen, even at ambient temperature, reaching 0.5 wt.% hydrogen (corresponding to MgNi₂H_{0.7}). This result demonstrated a feasibility method of optimizing the hydriding property of a MgNi₂-based system by nanostructuring.

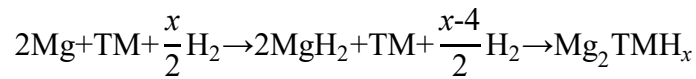
(2) Mg-Fe alloys

The hydride Mg₂FeH₆ can be produced upon reacting with hydrogen (according to the reaction Eq. (1)) despite the lacking miscibility of Mg and Fe.[44]



In particular, Mg₂FeH₆ is promising as a hydride on account of its outstanding volumetric and gravimetric hydrogen storage capacities, reaching 150 kg/m³ and 5.5 wt.%, respectively. In particular, Mg₂FeH₆ possesses an extremely high hydrogen concentration per unit volume (9.1×10^{19} atoms⁻¹), which exceeds the figure of MgH₂ (6.5×10^{19} atoms⁻¹) by around 40%.[45] Whereas in terms of the theoretical stability, Mg₂FeH₆ holds the relatively high enthalpy of dissociation (98 kJ (mol⁻¹ H₂)), which is a drawback for the real energy storage applications. Besides, the disproportionation occurs during the desorption process, where Mg₂FeH₆ decomposes into Mg and Fe

accompanied by the release of hydrogen. The release of hydrogen was reported to be declined apparently after four successive cycles. Notably, Batalovic[46] demonstrated that the addition of transition metal (Ni, Co, and Mn) attained a modification of the hydrogen sorption properties of Mg_2FeH_6 . The maximum reduction in desorption enthalpy of $27.7 \text{ kJ (mol}^{-1} \text{ H)}$ was achieved in the case of Ni doping. Similar to the Mg-Fe system, Mg_2CoH_5 (hydrogen storage capacity, 4.5 wt.%) formed as long as mechanical mixing elemental Mg and Co under a hydrogen atmosphere, of which the hydride synthesis enthalpy is $-82 \text{ kJ (mol}^{-1} \text{ H}_2)$, dehydrogenation temperature is $\sim 513 \text{ K}$ under 1 bar hydrogen pressure.[47] Specifically, the production of Mg_2FeH_6 comprises two stages where MgH_2 regularly adopted as a precursor. More specifically, MgH_2 is first formed after a certain period of the ball-milling process, and then it further reacts with Fe to produce Mg_2FeH_6 as prolonging the milling time. Mg_2FeH_6 , however inversely produces metal and hydrogen in one-step way, supported by the *in-situ* hydrogen desorption curve (Figure 3) observed throughout the formation of Mg_2TM (TM = Fe and Co) hydrides based on the reaction equation (Eq. (2));[48] Meanwhile, a novel absorption stage was noticed with regard to Ni.[49]



(For Fe, Co, $x = 6, 5$) (2)

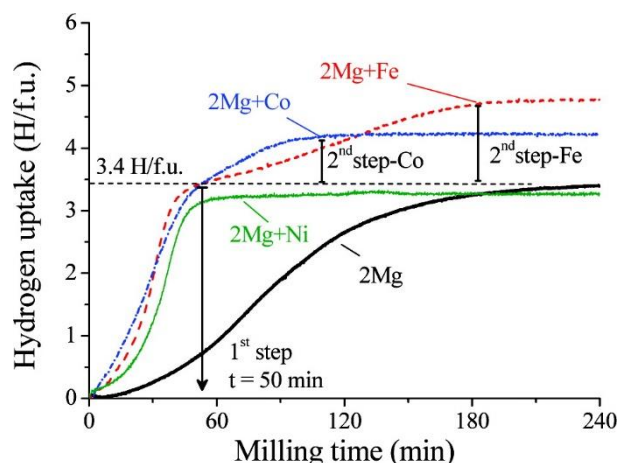


Fig. 3. Absorbed hydrogen atoms by formula unit of the formed hydride during RBM of Mg and Mg^{+2}TM mixtures (TM = Ni, Fe, and Co) (The number of absorbed H atoms per unit metal or alloy formula (H/ f.u.)). Reproduced by permission from Zhang *et al.*, J. Phys. Chem. C 115, 4971 (2011). Copyright 2011 by ACS publications.

2.1.2 Mg-based hydrogen alloys with one-step disproportionation reaction

The hydrogen involving the reaction process is complex in some Mg-based hydrogen storage alloys. For example, it has been found that a disproportionation reaction, i.e., $\text{MgB} + \text{H} \rightarrow \text{MgH}_2 + \text{B}$, might be caused during the hydriding of these alloys. Notably, MgH_2 hydride is so stable that the onset of this reaction is undesirable, because it makes the hydrogen desorption reaction very difficult. According to the reaction pathway, we will mainly introduce two representative Mg-based hydrogen alloys with one-step disproportionation reaction in this section (i.e., Mg-RE alloys and Mg-transition metal systems). Then, three another typical Mg-based hydrogen alloys with multi-step disproportionation reaction (i.e., Mg-Ba, Mg-Ca, and Mg-Ga alloys) will be reviewed in section 2.1.3.

(1) Mg-RE alloys

Since the 1970s, Mg-based hydrogen storage alloys without adding Ni but covering

almost all other metallic elements and a few nonmetallic elements, have been widely studied. In this case, Mg-based alloys can be formed from Mg and more than two non-Ni elements. Besides, since the 1980s, Mg and lanthanide RE alloys (e.g., REMg_{12} , REMg_{17} and $\text{RE}_5\text{Mg}_{41}$) have also been studied extensively because Mg and lanthanide RE metals can form the relatively stable alloy. However, Mg-RE alloys are proved impractically to apply due to the high hydrogen absorption/desorption temperature albeit the noticeable hydrogen storage capacity of those compounds. Taking $\text{La}_2\text{Mg}_{17}$ as an example, which holds a storage capacity of around 6 wt.%, it can only absorb hydrogen at nearly 350 °C.[50] Moreover, $\text{La}_2\text{Mg}_{17}$ transforms into LaH_3 and MgH_2 upon the hydriding process, where the LaH_3 is irreversibly bound.

Notably, a Mg_3RE type compound (Mg_3La) with a D03 type structure (BiF_3 type, space group $\text{Fm}\bar{3}\text{m}$) was thereafter reported. Mg_3LaH_9 hydride, owning an unrecognized crystal structure so far and a hydrogen storage capacity of 4.1 wt.% in theory, was formed under extremely high pressure (5 GPa).[51] Accordingly, Ouyang *et al.*[52] initially reported the hydrogen storage properties of D03 structured Mg_3La alloy that was prepared by induction melting. It was found that the Mg_3La alloy can react easily with hydrogen for the formation of metallic hydride at ambient temperature and under 1 atm pressure, possessing a reversible hydrogen storage capacity of about 2.89 wt.%. However, the release of hydrogen from the Mg_3La hydride arises at a rather high temperature, denoting the lowest temperature as high as 274 °C. In addition, many types of Mg_3RE compounds with the D03 structures can be synthesized by induction melting. The maximum reversible hydrogen absorption capacities of various Mg_3RE , e.g., Mg_3La , [52] Mg_3Pr , [53] Mg_3Nd , [54, 55] and Mg_3Mm [56, 57] alloys are 2.89 wt.%, 2.58 wt.%, 1.95 wt.% and 2.91 wt.%, respectively, according to their PCI curves. The D03 structured Mg_3RE compounds transform into FCC structured phases after the

hydrogenation processes. All the hydriding of these alloys are occurred at ambient temperature together with speedy hydrogenation/dehydrogenation kinetic properties. The nanometer-sized REH_x phase has been found to be *in situ* formed upon activation, showing a beneficial catalytic effect on accelerating the kinetics. Further increased kinetics were obtained via mixing transition metals, especially Ni and Co, with Mg₃RE.[34, 56-58] For example, it has been proved that Mg-RE-Ni alloy performs well during the hydriding process, which is attributed to the thermodynamic modification of the addition Ni.[34, 59, 60] Besides, the synthesis of fine REH_x precipitates by adding the RE elements can catalyze the hydrogen desorption of MgH₂. [52, 53, 55, 61]

(2) Mg-transition metal systems

Mg-Cu alloys: Mg acquires two types of intermetallic compounds upon alloying with Cu, viz. Mg₂Cu and MgCu₂, [62] of which Mg₂Cu alloy can easily react with hydrogen at 300°C under 2.15 MPa hydrogen pressure. While MgCu₂ barely absorbs hydrogen although heating to 350°C under 2.35 MPa hydrogen pressure. [63] Meanwhile, Mg₂Cu can also reversibly undergo hydrogenation by forming two products via disproportionation (Eq. (3)), which is different from Mg₂Ni by forming a single hydride (Mg₂NiH₄). [63]



The hydrogenation temperature of Mg₂Cu alloy can be reduced to about 240 °C under 1 bar hydrogen pressure. Unfortunately, this reaction becomes irreversible. Such a reaction displays modified thermodynamics ($\Delta H_d = 70 \text{ kJ (mol}^{-1} \text{ H}_2\text{)}$) as well. MgH₂ may interact with MgCu₂ and generate Mg₂Cu. Thus, the modified or substituted Mg₂Cu alloys can be achieved. Additionally, it has been proved that the Mg-Cu-H nanoparticle system possesses modified thermodynamics: the hydrogenation enthalpy

and entropy are improved to be $-67.5 \text{ kJ (mol}^{-1} \text{ H}_2\text{)}$ and $-124.4 \text{ J (K}^{-1} \text{ mol}^{-1} \text{ H}_2\text{)}$, respectively.[64]

When the concentration of Mg in the alloy exceeds the normal composition corresponding to Mg_2Cu , the PCI curve of this Mg-Mg₂Cu alloy exhibits two plateaus and enhanced hydrogen storage properties, which closely resembles the Mg-Mg₂Ni system.[34] For example, the alloy consisting of 90.5 wt.% Mg together with 9.5 wt.% Cu can react quickly with hydrogen at a temperature lower than 300°C under pressure of 3 MPa, achieving an exceptional hydrogen storage content over 6.62 wt.%. Accordingly, the upper plateau is attributed to the interaction of hydrogen and intermetallic compound, i.e., Mg₂Cu with hydrogen.[63] Besides, it's worth noting that the existing Mg₂Cu in two-phase Mg-Mg₂Cu alloy catalyzes the reaction between hydrogen and Mg, in comparison with the higher hydrogenation pressure and temperature of single-phase Mg alone.[65, 66] This has also been confirmed by thermodynamics and surface research. As shown in Figure 4, they concluded that the outside Mg surface exposes to oxygen and forms an oxide layer, conversely, the interface between Mg and Mg₂Cu is out of touch with oxygen leading to a lack of barrier. Therefore, it was assumed in their models that in contrast to that of Mg, the external surface of Mg₂Cu retains its capability to liberate hydrogen which is released to the underlying Mg afterward. Hence, it was proposed that hydrogen tends to hinder Cu from reacting with oxygen but not impeding Mg.[45] Furthermore, the decomposition of MgH₂ in two-phase Mg-Mg₂Cu alloy with the existence of Mg₂Cu is fairly quick, especially at the larger H/Mg ratios, where the equilibrium dissociation pressures can be achieved even at 275°C.

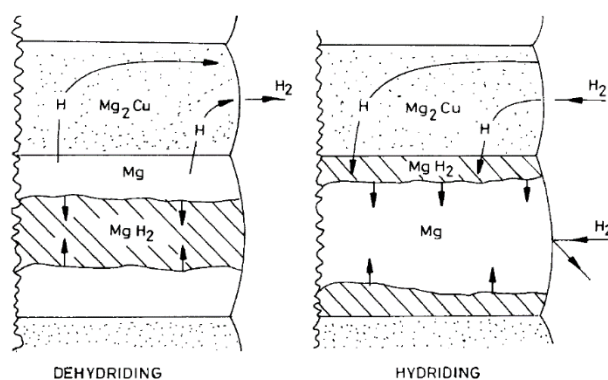


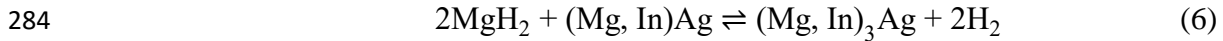
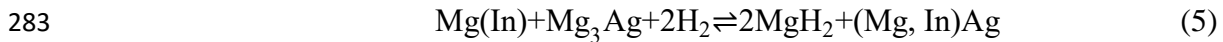
Fig. 4. Hydriding and dehydriding model of Mg_2Cu catalyzed Mg . Reproduced by permission from Selvam *et al.*, Int. J. Hydrogen Energy 11, 169 (1986). Copyright 1986 by Elsevier.

Mg-Ag alloys: Douglass[67] has investigated the reaction behaviors between hydrogen and $Mg-Ag$ alloys with Ag concentration ranging between 1-5 at.%. The noticeable points of the hydrogenation and dehydrogenation behaviors of Mg -transition metal alloys are listed in Table 1. These data indicate the effects of Ag on the dehydrogenation process in comparison with the remarkable systems, like $Mg-Ni$ and $Mg-Cu$. Besides, it is interesting to note that the hydrogen storage properties of Mg_3Ag have also been investigated.[68, 69] Similar to $Mg-Cu$ alloys, the reversible Mg_3Ag-H_2 system undergoes the hydrogenation via the reaction in Eq. (4), which possesses a lower ΔH_d value (69.8 kJ/mol H_2).[70]



The results in Table 1 obviously display that mixing Mg with other metals generates Mg -based alloys that can effectively enhance hydrogenation and dehydrogenation thermodynamics. In addition, the effect of the solid solution on the hydrogen storage properties of Mg -based compounds has been studied. For example, Si *et al.*[71] fabricated the $Mg_{5.7}In_{0.3}Ag$ alloy by casting, founding that this alloy formed by mixing

282 Mg(In) solid solution and Mg₃Ag compound with the following reactions (Eq. (5-6)):



285 This study confirmed that the (Mg, In)₃Ag-H₂ system can alter the thermodynamics
 286 ($\Delta H_d = 62.6 \text{ kJ (mol}^{-1} \text{ H}_2\text{)}$), which was attributed to the dual destabilization by adding
 287 Ag as well as the dissolution of In. Particularly, the solid solution of In introduces the
 288 catalytic effect to enhance the hydrogen desorption from additional MgH₂. As indicated
 289 by decreased activation energy (78.2 kJ mol⁻¹), Mg_{5.7}In_{0.3}Ag showed the faster
 290 hydrogen desorption kinetics than that of the Mg₆Ag sample.

291 Table 1. Hydrogen absorption and desorption behavior of various Mg-transition metal
 292 alloys.

Alloy composition (atomic%)	Hydrogen content (wt.%)	Hydriding conditions		Hydrogen released (wt.%)	Dehydriding	
		Pr.	Temp.		Pr.	Temp.
		(atm)	(°C)		(atm)	(°C)
Mg ₂ Ni	3.6	25	350	—	—	—
Mg-Mg ₂ Ni	5.7	25	350	—	—	—
Mg ₂ Cu	2.7	30	300	—	—	—
Mg-Mg ₂ Cu	6.6	30	300	—	—	—
Mg ₂ Fe*	5.4	20-120	450-520	—	—	—
Mg-Mg ₁₇ Y ₁₃	5.0	10	400-450	4.5	3.0	320
Mg-1Y	4.5	56	400	4.0	1.0	300
Mg-5Y	7.0	56	400	3.4	1.0	300
Mg-5Mn	6.0	56	400	1.5	1.0	300
Mg-5Co	2.0	56	400	0.0	1.0	300
Mg-1Ag	5.7	56	400	2.0	1.0	300
Mg-5Ag	5.3	56	400	0.0	1.0	300
Mg-1Ag-1Y	6.0	56	400	—	—	—

Mg-1Ag-1Y	6.3	56	400	—	—	—
Mg-5Ni-5Y	5.2	56	400	3.1	1.0	300
Mg-5Al-5Y	5.0	56	400	3.1	1.0	300
Mg-10Al-10Y	4.1	43	400	—	1.6	310
Mg-34Al-10Y	3.6	43	400	—	2.2	310
					1.0	286
Mg-10Cu-5Ni-	3.7	21	400	—	2.0	310
					1.5	299
Mg ₈₀ Ag ₁₅ Al ₅	1.7				2.2	300
Mg ₈₅ Ag ₅ Al ₁₀	3.8				2.6	300
Mg ₉₀ Ag _{7.5} Zn _{2.5}	4.2				2.8	300
Mg ₇₈ Ag _{16.5} Zn _{5.5}	2.5				2.8	300

293

294 Besides, Mg-Ag-Me ternary alloys have also been investigated. For example, Lu *et*
295 *al.* fabricated Mg-Ag-Al[72], Mg₈₀Ag₁₅Al₅ and Mg-Ag-Zn [73] alloys and revealed that
296 their reaction routes differ from that in pure Mg. An intermediate phase, comprising a
297 new ternary solid solution MgAg(Al), was found to react with MgH₂ during the
298 dehydrogenation process, thus leading to an rise in the hydrogen desorption equilibrium
299 pressure (0.22 MPa at 300 °C) with a reversible hydrogen storage capacity of 1.7 wt.%.
300 The compositional adjusted Mg₈₅Ag₅Al₁₀ can possess a reversible hydrogen storage
301 capacity of about 3.8 wt.% and an increased equilibrium pressure (0.26 MPa at 300 °C).
302 In addition, a large fraction of phase boundaries were found to be existed in the
303 hydrogenated Mg-Ag-Zn alloys, which were prepared by ball milling MgH₂ with
304 Ag(Zn) solid solution, contributing to more hydrogen diffusion channels.

305 2.1.3 Mg-based hydrogen alloys with multi-step disproportionation reaction

306 Different from Mg-based hydrogen alloys with one-step disproportionation
307 reaction, Mg-based hydrogen alloys with multi-step disproportionation reaction, such
308 as Mg-Ba alloys, Mg-Ca alloys, and Mg-Ga alloys, means this type of materials
309 contains more than one hydrogen desorption processes for forming the hydrides.

(1) Mg-Ba alloys

Ab initio calculations were adopted by Bhihi and collaborators[74] which predicted that modifying MgH_2 with a small quantity of alkaline metals (Sr, Ba) could reduce remarkably the stability of MgH_2 . Mg-Ba system comprises various types of alloys (e.g., $\text{Mg}_{17}\text{Ba}_2$, $\text{Mg}_{23}\text{Ba}_6$, and Mg_2Ba). [75] Wu *et al.* [76] investigated the hydrogen storage properties and phase transition mechanisms of $\text{Mg}_{17}\text{Ba}_2$ alloy via induction melting. The reversible hydrogen storage content of $\text{Mg}_{17}\text{Ba}_2$ alloy is about 4.0 wt.%. The PCI curves of $\text{Mg}_{17}\text{Ba}_2$ are displayed in Figure 5 and the dehydrogenation pathway with three steps can be expressed in Eq. (7-9) as follows:

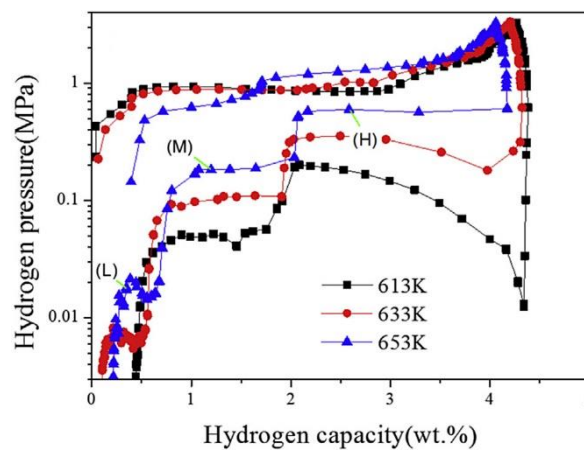


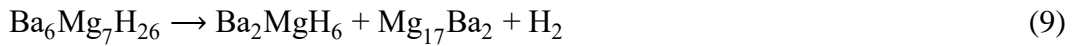
Fig. 5. PCI curves of $\text{Mg}_{17}\text{Ba}_2$ compound measured at different temperatures. Three points (H), (M), and (L) are indicated in the PCI curves. Reproduced by permission from Wu *et al.*, J. Alloys Compd. 690, 519 (2017). Copyright 2017 by Elsevier.



Medium platform:



Low platform:



The hydrogen desorption activation energy of $\text{Mg}_{17}\text{Ba}_2$ was verified to be 173.92 kJ/mol. Moreover, the dehydriding thermodynamics data of $\text{Mg}_{17}\text{Ba}_2$ at different platforms are listed in Table 2.

Table 2. Dehydrogenation enthalpy and entropy change of $\text{Mg}_{17}\text{Ba}_2$ compound at different platforms. Reproduced by permission from Wu *et al.*, J. Alloys Compd. 690, 519 (2017). Copyright 2017 by Elsevier.

Temperature (K)	ΔH (kJ (mol ⁻¹ H ₂))	ΔS (J (K ⁻¹ mol ⁻¹ H ₂))
High platform	88.9	150.9
Medium platform	107.9	170.3
Low platform	165.8	240.9

(2) Mg-Ca alloys

Chiotti et al [77] proved that CaMg_2 could interact with hydrogen and then convert to CaH_2 and elemental Mg at 450 °C. Meanwhile, the hydrogen storage capacity of CaMg_2 alloy is hopeful to exceed 6.3 wt.%, with the H/M ratio of 2. Adding Ni to Mg-based alloys is widely applied to catalyze hydrogen on the Mg surface when the hydrogenation process moves forward. Then several CaMg_2 -based alloys associated with Ni have been found to show outstanding hydrogen storage capacities. For example, Lupu *et al.*[78] found that $\text{CaMg}_{1.8}\text{Ni}_{0.5}$ alloy possesses 5.7 wt.% hydrogen storage capacity at 338 °C with rapid hydriding kinetics. Terashita *et al.*[79] reported that $(\text{Ca}_{0.8}\text{La}_{0.2})\text{Mg}_{2.2}\text{Ni}_{0.1}$ alloy could absorb 5.1 wt.% hydrogen even at ambient temperature. To improve the hydrogen capacity and reduce costs of CaMg_2 -based alloys,

Ma *et al.*[80] designed a $\text{CaMg}_{1.9}\text{Ni}_{0.1}$ alloy by adding a small quantity of Ni through induction melting. The experimental results showed that the addition of Ni enables the $\text{CaMg}_{1.9}\text{Ni}_{0.1}$ alloy to have a room-temperature absorption of hydrogen under mild hydrogen pressure, reaching the hydrogen storage content of 5.65 wt.% and distinct activation energy of 41.74 kJ/mol.

(3) Mg-Ga alloys

There are a lot of intermetallic compounds included in the Mg-Ga alloy system (e.g., Mg_5Ga_2 , Mg_2Ga , and MgGa). The solid solubility of Ga in Mg-Ga alloy system reaches 5 wt.% at temperature of 573 K,[81] and a $\text{Mg}(\text{Ga})$ solid solution can be generated during the hydriding/dehydriding process of Mg-Ga alloy. For instance, Wu *et al.*[82] prepared the solid solution expressed as $\text{Mg}(\text{Ga})$ at a rather high temperature and found that the $\text{Mg}(\text{Ga})$ solid solution creates reversible hydrogen-absorbing capacity (5.7 wt.%) for Mg-Ga alloy. The (de)hydrogenation process of intermetallic compounds, such as the Mg_5Ga_2 compound, was found to be reversible with the reaction expressed as Eq. (10):



While the hydrogen desorption process of the Mg-Ga hydrides consists of two steps: the first one is the combination of Mg_2Ga with MgH_2 to produce Mg_5Ga_2 and liberate H_2 simultaneously; the second step involves the transformation of MgH_2 to Mg and H_2 . Especially, the reaction occurred in the first step improves the whole dehydriding process and decreases the dehydriding enthalpy. The dehydriding enthalpy and activation energy of the Mg-Ga alloy are proved to be 68.7 kJ/mol H_2 and 149 kJ/mol, respectively. When comparing to the pure Mg enthalpy (77.1 kJ/mol H_2), it is obvious noted that Mg-Ga alloy has improved the dehydrogenation thermodynamic properties.

2.2 Solid solutions

Generally, alloying to form the intermetallic compounds is an achievable method to improve the thermodynamic properties of Mg-base hydrogen storage alloys. But there are some weaknesses yet, such as the decrease in the hydrogen capacity due to the heavy alloying metallic elements and the poor reversibility resulted from the broken bonds between Mg and other metallic elements during the hydriding reaction. Besides, most of the intermetallic compounds, such as Mg-Fe, Mg-Co, and Mg (In, Cd), possess the higher ΔH for the dehydriding process than that of Mg/MgH₂. Hence, further study should be carried out to solve these remaining problems.

Alternatively, constructing an Mg-based solid-solution alloy is believed to be a destabilization strategy, which can slightly modulate the structure and composition of Mg at the expense of moderate capacity, thus likely adjusting the thermodynamic stability. Especially, Cd is the exclusive element expressing unlimited solid-state solubility in Mg. In this regard, Douglass *et al.*[67] firstly covered the Mg-1 at.% Cd solid solution, which presents a 5 wt.% hydrogen storage content at 673 K in 24 h. Besides, Schulz[83] comprehensively studied the hydriding kinetic and thermodynamic properties of Mg-x at.% Cd (x = 5, 10, and 20) alloys, which are extremely difficult to activate for the hydrogen absorption even after annealing at temperature of 523 K for 24 h under 1.5 MPa hydrogen pressure. Interestingly, Skripnyuk *et al.*[84] synthesized Mg₃Cd alloys via high-energy mechanical milling, which displays a reversible hydrogen storage content of 2.8 wt.% along with a 2.5 wt.% hydrogen storage capacity at the temperature of 573 K in 120 s. Fortunately, there is no measurable pressure hysteresis detected from the PCT curve of Mg₃Cd shown in Figure 6 with a hydrogenation enthalpy of -65.5 kJ mol⁻¹.

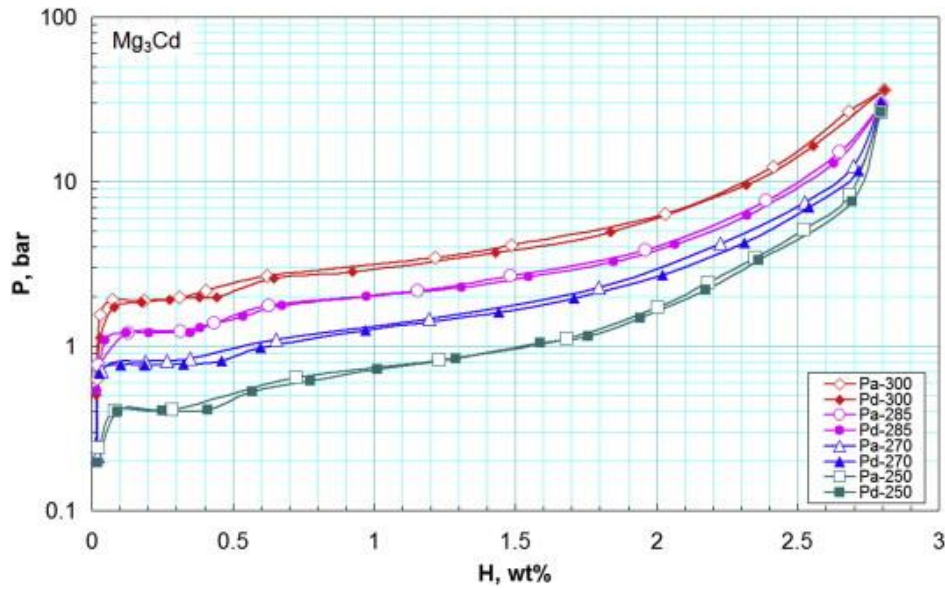


Fig. 6. PCT curves of the studied Mg_3Cd alloy at temperature ranging 250-300 °C. The open and filled symbols correspond to the absorption and desorption branches of the curves, respectively. Reproduced by permission from Skripnyuk *et al.*, Int. J. Hydrogen Energy 37, 10724 (2012). Copyright 2012 by Elsevier.

On the basis of the binary phase diagram belonging to the Mg-In system, it could also possess a considerable solubility up to 10 at.% within a wide range of temperatures.[45, 85, 86] The reversible formation of Mg (In) solid solution supplies an effective strategy to modulate the dehydrogenation thermodynamic properties of MgH_2 . The Mg (In) solid-solution alloys absorb hydrogen and generate MgH_2 together with disordered Mg-In compounds. The corresponding lattice constants, as well as hydrogen storage capacities of Mg (In) solid-solution, are summarized in Table 3. The $\text{Mg}_{0.95}\text{In}_{0.05}$ solid-solution alloy can reversibly react with hydrogen at temperature of 573 K according to the following equation (Eq. (11)):



The hydrogen storage content of $\text{Mg}_{0.95}\text{In}_{0.05}$ is up to 5.3 wt.%, while it owns sluggish

kinetic property in the hydrogenation/dehydrogenation process.[87] Accordingly, Zhu *et al.*[88] added some other elements to synthesize ternary Mg-based solid-solution alloys, involving Mg (In, Al), Mg (In, Cd) and Mg (In, Y) alloys. Mg (In, Al) ternary solid solution indicates the modified dehydriding reversibility as well as a significant reduction of ΔH when comparing to the binary Mg (Al) solid solution, owing to the dissociation of Al in the β phase.

In terms of the Mg-In-Y ternary system, a reversible solubility of Y in Mg could be obtained upon decomposing the In_3Y phase during dehydrogenation, while the reversible dissolving of Y is relatively deficient attributing to the production of YH_2 . The $\text{Mg}_{90}\text{In}_5\text{Y}_5$ alloys exhibit a reduced hydriding enthalpy of $62.9 \text{ kJ (mol}^{-1} \text{ H}_2\text{)}$, which is decreased by $5 \text{ kJ (mol}^{-1} \text{ H}_2\text{)}$ and $12 \text{ kJ (mol}^{-1} \text{ H}_2\text{)}$ when comparing to the figures of the $\text{Mg}_{95}\text{In}_5$ binary solid solution alloys and pure Mg, respectively.[89] The hydrogenation process of the $\text{Mg}_{90}\text{In}_5\text{Cd}_5$ alloy resembles the Mg-In-Y system, which can be expressed as the following equation (Eq. (12)):

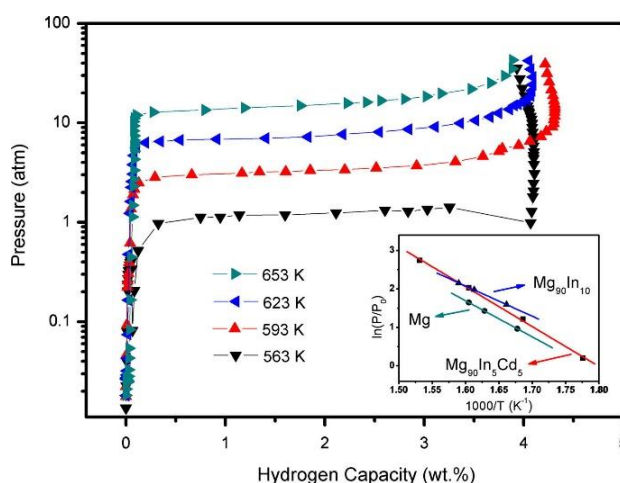
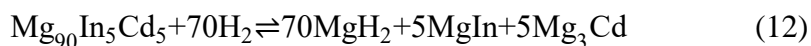


Fig. 7. PCT and Van't Hoff plot (the inset) for the hydrogen desorption of the $\text{Mg}_{90}\text{In}_5\text{Cd}_5$ alloy. Reproduced by permission from Lu *et al.*, J. Alloys Compd. 645,

427 S103 (2015). Copyright 2015 by Elsevier.

428 Table 3. Lattice constants of Mg-based solid solutions and their hydrogen storage
429 properties. Reproduced by permission from Zhang *et al.*, RSC Adv. 9, 408 (2019).
430 Copyright 2019 by RSC publications.

Solid solution	Lattice constants (nm)		$ \Delta H $	ΔS	Capacity
	a	c	(kJ (mol ⁻¹ H ₂))	(J (K ⁻¹ mol ⁻¹ H ₂))	(wt.%)
Mg _{0.9} In _{0.1}	0.31929	0.52061	65.2	121.8	4.2
Mg _{0.95} In _{0.05}	0.32027	0.52086	68.1	125.5	5.3
Mg _{0.98} In _{0.02}	0.32077	0.52106	69.6	126.0	6.4
Mg _{0.75} Al _{0.25}	0.31990	0.51960	76.8	138.6	5.0
Mg _{0.9} In _{0.05} Al _{0.05}	0.31980	0.51929	66.3	121.2	4.8
Mg ₉₀ In ₅ Cd ₅	0.31925	0.51964	86	154.8	4.3

431 The dehydrogenation enthalpy (ΔH) and entropy (ΔS) of the Mg₉₀In₅Cd₅ alloy are 86.0
432 kJ (mol⁻¹ H₂) and 154.8 J (K⁻¹ mol⁻¹ H₂), respectively. The PCT curves indicate a
433 reversible hydrogen storage content of 4.3 wt.% as well as a raised equilibrium pressure
434 of MgH₂ in Mg₉₀In₅Cd₅ alloy compared with that of pure MgH₂ (Figure 7). The
435 Mg₉₀In₅Cd₅ alloy exhibits an improved hydriding kinetic property and a reduced
436 hydriding activation energy of 61.0 kJ mol⁻¹ as well, while the hydrogen desorbing rate
437 is tardy as a result of the long-range diffusion of In and Cd in MgH₂. [90]

438 2.3 Other compounds

439 MgH₂ generating from ball milling proceeds a serious growth in crystallite size or
440 subsequent structural relaxation of defects upon the very first hydrogen cycle, which
441 slowly shrinks the benefit of nanocrystallization. Therefore, it urgently desires an

appropriate approach to preserve nanoparticles from aggregation or recrystallization. It has been found that pure Mg embedded in 2D or 3D material could prevent the growth of nanoparticles. In this regard, Mg nanoparticles limited in carbon aerogels (CA) have appealed to much attention.[91-93] For example, Liu *et al.*[92] reported that Mg nanoparticles confined in carbon aerogels via the hydriding process of infiltrated dibutyl-Mg followed by hydrogen release at 623 K, which has a size in the range of 5.0 to 20.0 nm. The hydrogenation and dehydrogenation enthalpies of the confined Mg were determined to be 65.1 ± 1.56 kJ (mol⁻¹ H₂) and 68.8 ± 1.03 kJ (mol⁻¹ H₂), respectively. Jia *et al.*[94] synthesized the MgH₂@CMK-3 nanoconfinement system and experimentally accomplished the low-temperature hydrogenation starting from 323 K. Comparing with the calculated reaction energy (E_r) from clusters of pure MgH₂ and MgH₂/C (Figure 8), they deduced that the interfacial effect can effectively increase the low-temperature dehydriding properties of MgH₂ clusters, even though the cluster is not ultra-small (Figure 8c). Accordingly, they presented a novel mechanism for destabilizing Mg-H bonding through the mix of the size effect and MgH₂-carbon scaffold interfacial bonding, which is more superior to nanoparticles or 2D films. The use of scaffolds impedes the particle enlargement and agglomeration, but it leads to a critical capacity loss. Hence, altered forms of stabilization should be searched to increase the storage capacity, while presenting adequate stabilization for nanosized Mg without scaffolds, such as the appending of modified graphene nanoribbons, the introduction of a second phase, reserving additional hydrogen and core-shell methods, should be conducted.

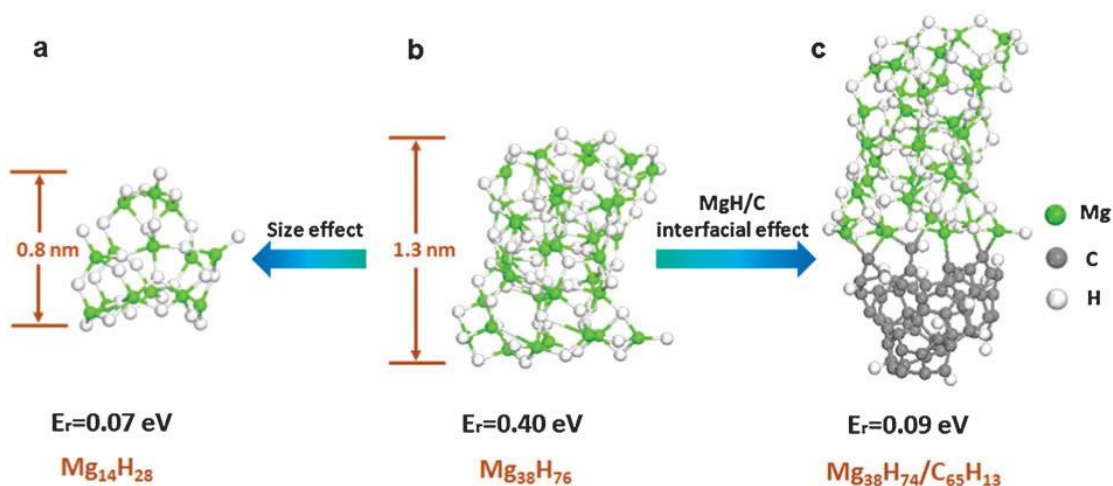


Fig. 8. Reaction energy (E_r) for hydrogen release from clusters of pure MgH₂ and MgH₂/C. (a) Pure Mg₁₄H₂₈ cluster; (b) Mg₃₈H₇₆ cluster; (c) Mg₃₈H₇₄ adsorbed on the cluster of amorphous carbon. Mg, C and H atoms are indicated by green, grey and white spheres, respectively. Reproduced by permission from Jia *et al.*, Phys. Chem. Chem. Phys. 15, 5814 (2013). Copyright 2013 by RSC.

In addition, Mg-based glasses or nanoglasses is also a new system that attracts extensive attention. For instance, Lin *et al.*[95] found that the Mg-Ce-Ni metallic glasses (MGs) can reversibly absorb and desorb about 0.2-0.4 wt.% H at room temperature without pre-activation, and the hydrogenation capacity of the glassy Mg-based alloy is twice as that of the corresponding crystalline alloy due to its free volume and disordered atomic structure. Recently, Lin *et al.*[96] continued to investigate the hydrogenation kinetics of two five-component Mg₆₀Ce₁₀Ni₂₀Cu₅X₅ (X = Co, Zn) metallic glasses under a hydrogen atmosphere. This work demonstrated that alloying with Zn leads to the negligible impact on the hydrogenation kinetics and storage capacity of the Mg-Ce-Ni-Cu metallic glass. However, alloying with Co can remarkably improve the hydrogenation kinetics and storage capacities. Apparent activation energies for the hydrogenation were calculated to be 64.4 kJ/mol, and 107.2

kJ/mol, respectively, for the $\text{Mg}_{60}\text{Ce}_{10}\text{Ni}_{20}\text{Cu}_5\text{Co}_5$ and $\text{Mg}_{60}\text{Ce}_{10}\text{Ni}_{20}\text{Cu}_5\text{Zn}_5$ metallic glasses.

3. Approaches to modifying the properties of Mg-based alloys

Mg-based alloys, considered as a potential candidate for hydrogen storage, possess a rather high dehydrogenating temperature and sluggish kinetic properties of their hydride MgH_2 , which blocks their practical applications. In this section, some particular effective approaches to modifying the kinetics and thermodynamics of Mg-based hydrogen storage alloys will be reviewed.

3.1 Kinetic modifying

In the past few decades, significant progress has been made in improving the hydrogenation/dehydrogenation kinetics of Mg-based alloys by nanostructuring, synthesizing metastable phases, doping catalytic additives and changing the reaction path. However, the tuning of their kinetic properties is still a great challenge. Herein, we present a summary of the recent advances and developments in enhancing the kinetics of Mg and Mg-based alloys.

3.1.1 Nanostructuring

It has been found that raising the densities of various defects, including grain/interphase boundary, dislocations, and stacking faults, etc., via nanostructuring is favorable to the hydrogenation/dehydrogenation kinetics of hydrogen storage alloys, without increasing cost and slightly reducing hydrogen storage capacity.[23, 97-100] On the other hand, the introduction of extra boundary/surface might also reduce the reaction enthalpy of Mg-H systems. Therefore, nanostructuring can be an effective strategy to dually tune the thermodynamics and kinetics of Mg-based hydrogen storage materials. For example, in the process of ball milling, one typical method for

505 nanostructuring, the impact of high-speed balls on the sample introduces the severe
506 plastic deformation, which subsequently results in the structural defects, increased
507 stress and increased free energy of the uniform-composition sample system. More
508 importantly, the decreased particle size of the sample during nanostructuring will lead
509 to the shortening of the required length of hydrogen diffusion path, increasing of the
510 specific surface area and nucleating sites of the metal hydrogenation reaction, which
511 are all beneficial to the boosting of hydrogenation and dehydrogenation kinetics of Mg-
512 based alloys.[101, 102]

513 Nanostructuring has been most systematically investigated regarding the Mg_2Ni
514 alloy among the Mg-based hydrogen storage alloys.[103, 104] For example, Mg_2Ni can
515 be protected by hydrogen from ball milling, during which hydrogen reacts with Mg_2Ni
516 alloy, denoting the hydrogen reserves of 1.6 wt.%. The ball-milled sample has a good
517 hydrogen absorption performance, with a hydrogen absorption temperature of 140 °C,
518 and a reduced hydrogen release temperature of 250 °C. Besides, Song *et al.*[105]
519 prepared Mg_2Ni alloy samples by means of mechanical ball grinding, melting and
520 sintering, which could release hydrogen at 270 °C.

521 Particularly, Zhang and his coworkers[19] presented an innovative strategy, namely
522 microencapsulated nanoconfinement, for the synthesis of a structure where the
523 monodispersed Mg_2NiH_4 nanoparticles are anchored onto the graphene layer surface
524 by the method of hydriding chemical vapor deposition (HCVD), as schematically
525 displayed in Figure 9. The as-formed material holds greater stability in structure and an
526 excellent dehydriding kinetic rate. In addition, the MgO coating layer with a thickness
527 of around 3 nm effectually divorces the nanoparticles from accumulating with each
528 other during hydrogenation/dehydrogenation cycles, bringing elevated thermal and
529 mechanical stability. Furthermore, the MgO layer displays exceptional gas-selective

permeability to hinder the further oxidation of Mg_2NiH_4 and available for the hydrogenation/dehydrogenation process as well. Consequently, extraordinarily low activation energy (31.2 kJ mol^{-1}) for the hydrogen release reaction is acquired.

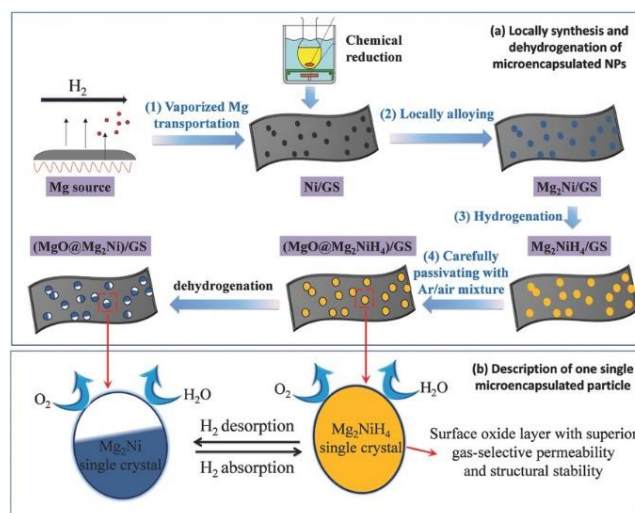


Fig. 9. Schematic of (a) the local synthesis of monodispersed Mg_2NiH_4 nanoparticles locally derived from Ni/GS by HCVD and the structural evaluation after hydrogen desorption. Reproduced by permission from Zhang *et al.*, Adv. Mater. 29, 1700760 (2017). Copyright 2017 by Wiley.

The mechanical alloying-induced nanostructuring can not only make powder particles more evenly distributed, but also refine grains, thus improving hydrogen storage kinetic performance. Therefore, nanostructuring of Mg-based alloys proposes a promising route to modify their kinetics meanwhile without an obvious decline in their hydrogen capacities. The formation of a nanocrystalline structure and associated defects through mechanical milling is often perceived as leading to enhanced hydrogen kinetics. Similarly to the case of surfaces discussed above, grain boundaries between nanocrystals contain excess energy, resulting in surface energy, thus providing another potential tool for reducing the reaction enthalpy of metal hydrides. In fact, the presence

of distinct types of lattice defects (grain boundaries, dislocations, stacking faults, and possible amorphization in some regions) that may likely act as either heterogeneous nucleation sites or diffusion pathways for hydrogen to be drawn away from the growing fronts and improve the hydrogen sorption characteristics subsequently.

The hydrogen release mechanism of bulk Mg_2NiH_4 with crystal defects and cracks was found that the hydride/metal transform from Mg_2NiH_4 to Mg_2NiH_x . As for the case of Mg_2NiH_x , Tran *et al.*[106] found a high density of various stacking faults in the dehydrided material (Figure 10). Note that similar results have also been reported in various alloy systems regarding the formation of defects in subsequent hydriding/dehydriding cycles. For instance, hexagonal closed-pack structured systems such as LaNi_5 [107] and FeTi [108, 109], have also been reported to possess the various defects, including vacancies, dislocations stacking faults, and a network of dislocations or deformation twins locating ahead of the Mg/MgH_2 interface.[110, 111] These defects-induced misfits are considered necessary to maintain the lattice coherency at the hydride/metal interphase and dissipate the accumulated elastic strain during the phase transformation. Specifically, stacking faults is greatly favorable for subsequent hydriding/dehydriding cycles, and it is therefore purposely introduced by severe deformation methods to facilitate the activation of hydrogen storage materials.[112] A variety of studies[113-118] also suggested that the formation of lattice defects such as grain boundaries, which can act as pathways for transportation of hydrogen through the oxide layer, can activate the material and then promote the kinetics of the hydrogen storage alloys.

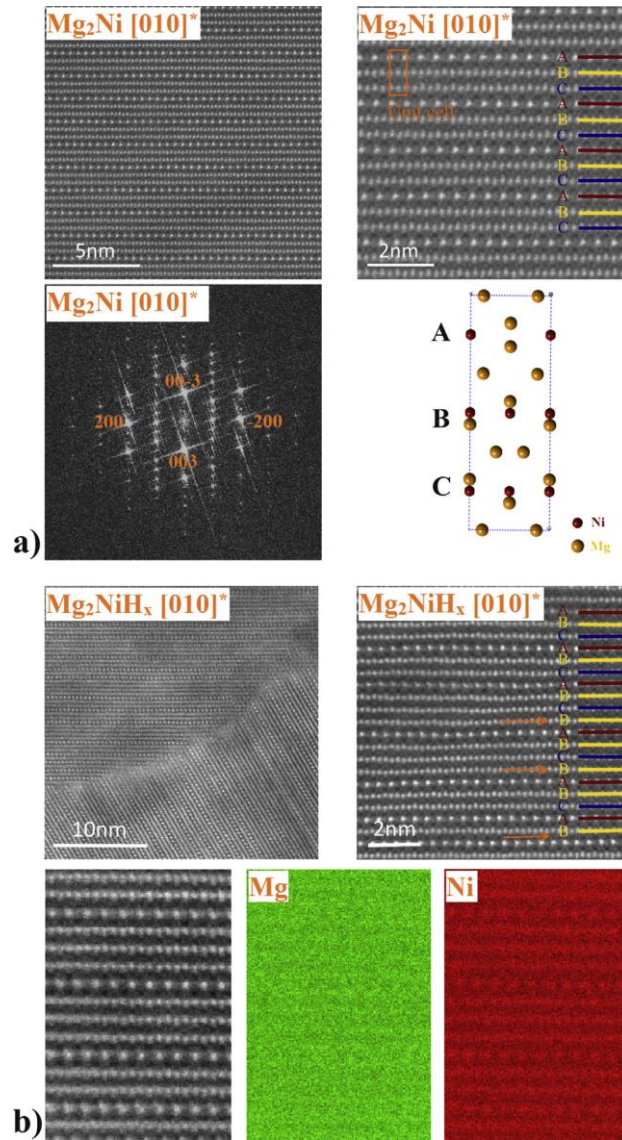


Fig. 10. a) Atomic-resolution images of the perfect unreacted Mg_2Ni lattice projected along $[010]$ zone axis and the corresponding atomic model, b) Atomic-resolution images of the adjacent dehydrided Mg_2NiH_x ($x \sim 0-0.3$) regions (along $[010]$ zone axis), showing a high probability of stacking faults (as indicated by the arrows) along with an EDS map. Reproduced by permission from Tran *et al.*, J. Power Sources 341, 130 (2017). Copyright 2017 by Elsevier.

3.1.2 Synthesizing metastable phases

The strategy of synthesizing metastable phases has been proved to modify the

kinetics of Mg-based hydrogen storage alloys. Specifically, the addition of early TMs (TM = Ti, Zr, Hf, V, Nb, and Ta) is helpful to stabilize the structure. A series of metastable Mg-rich $\text{Mg}_{6-7}\text{TMH}_{12-16}$ hydrides with CaF_2 related structure, have been synthesized, [119, 120] which can desorb 4.7 wt.% of hydrogen at 330 °C but decomposes into Mg and TiH_2 , but still require extremely high hydrogen pressure in the rehydrogenation process. Calizzi *et al.*[121] prepared Mg-Ti nanostructured samples containing a metastable Mg-Ti-H fcc phase, finding that the mean crystallite sizes of Mg and $\beta\text{-MgH}_2$ are both decreased with the increase in Ti content (Figure 11). Their results only showed the enhanced kinetic properties in the Mg-Ti system. Another research showed that the hydriding enthalpy of Mg-Fe-based materials with a crystallite size of 10 nm can be decreased by 6 kJ (mol⁻¹ H₂) between 523 K and 673 K.[122]

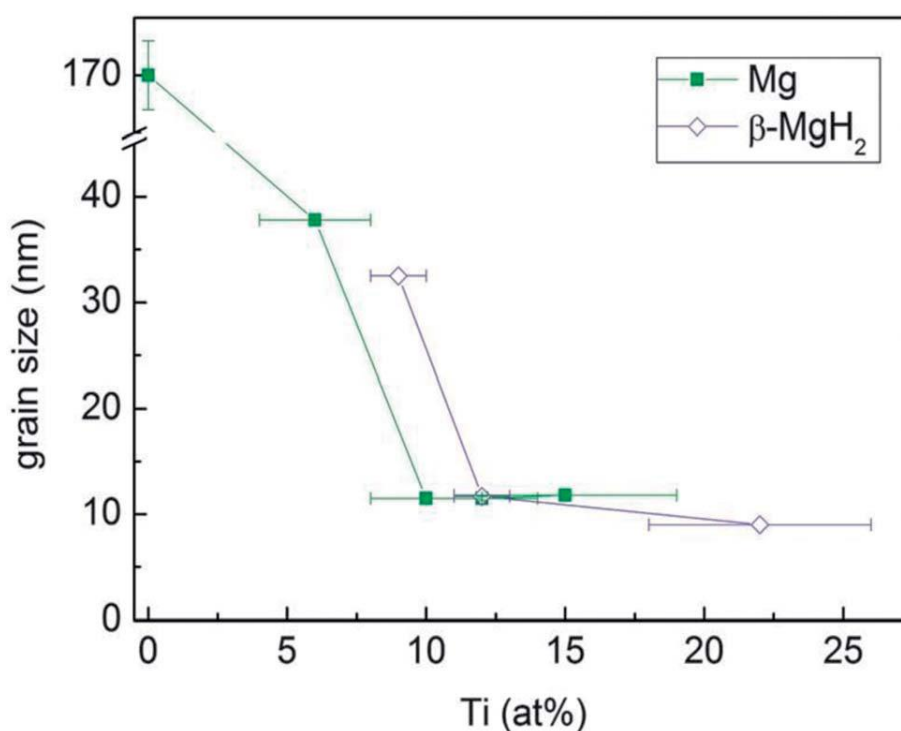


Fig. 11. Mean crystallite size of the Mg and $\beta\text{-MgH}_2$ phases in the Mg-Ti and Mg-Ti-H samples as a function of Ti content. Reproduced by permission from Calizzi *et al.*, Phys. Chem. Chem. Phys. 18, 141 (2016). Copyright 2016 by RSC.

The metastable nanostructured Mg-based alloys formed by the mechanical alloying approach might effectively solve the sluggish kinetics issue, as widely investigated by Shao and his coworkers.[59, 60] A considerable quantity of defects along with plastic deformation during mechanical alloying processes might result in the phase transitions in the synthesized Mg-based metastable nanostructured alloys, e.g., forming the BCC crystal structures with the characteristic performance of preserving the initial lattice structure during hydrogenation and dehydrogenation processes. Particularly, a summary of different Mg-based metastable nanostructured alloys with BCC lattice structure has been conducted by Shao,[123] especially the Mg-Co based metastable nanostructured alloys with BCC crystal structures. For example, Shao *et al.*[9, 124] reported Mg₅₀Co₅₀ and Mg₅₅Co₄₅ metastable BCC alloys with hydrogen storage values of 2.67-3.24 wt.% at 258 K, which is the lowest hydrogenation temperature for Mg-based materials described in the literature. Notably, Mg-Co BCC alloys possess a theoretical hydrogen storage content up to 20 wt.% in terms of geometrical calculation, albeit it is impossible to completely obtain up to date.

More specifically, Shao and his coworkers [125] explored the phase and morphology evolutions of ball-milled metastable nanostructured Mg-based Mg₅₀Co₅₀ hydrogen storage alloys with various milling durations as well. Co was found to be dispersed on the surface of Mg particles upon the start of milling, which is gradually cracked into a smaller size. After milling for 25 h, the FCC Co phase is synthesized, then the Co particles are dissolved into Mg particles. As the milling time prolongs to 50 h, the Mg particle size is markedly minished and the structure shifts to the BCC phase after 45 h. After 100 h milling, only one single BCC phase can be characterized, as shown in Figure 12. Moreover, differential scanning calorimetry (DSC) curves of both 50 h-, and 100 h-milled Mg₅₀Co₅₀ alloys showed two clear exothermic peaks,

which move to higher temperatures as milling time increasing due to the less amount
 of remaining catalytic Co phase. A widen exothermic peak including two overlapped
 peaks were observed in the 300 h-milled sample, which may be resulted from the
 welding on the particle surface during further milling, leading to fewer defects and less
 surface area on the surface. In terms of hydrogen storage properties, it was proved that
 the 100 h-milled $\text{Mg}_{50}\text{Co}_{50}$ alloy can react with more hydrogen at 258 K than that at a
 higher temperature of 323 K, as shown in Figure 13. The hydrogenation process
 detected by PCT measurements was thermodynamically dominant. The 50 h-milled
 $\text{Mg}_{50}\text{Co}_{50}$ alloy presented superior kinetics and hydriding capacity than that of 100 h-
 milled $\text{Mg}_{50}\text{Co}_{50}$ alloy, owing to the catalytic effect of remained Co in the 50 h-milled
 sample.

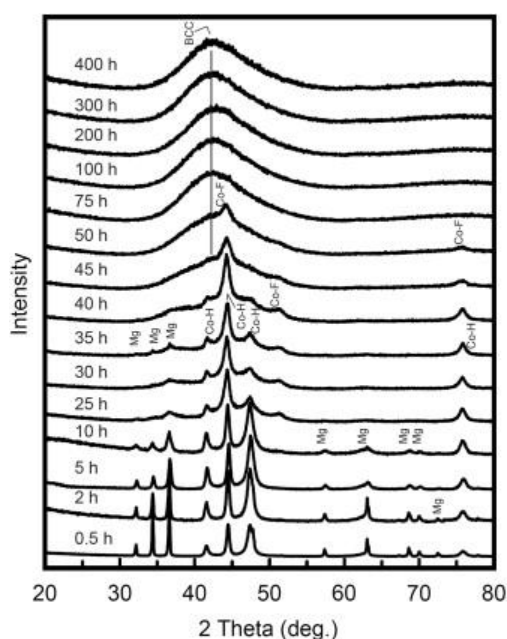


Fig. 12. XRD patterns of $\text{Mg}_{50}\text{Co}_{50}$ alloys ball milled for various periods. Reproduced
 by permission from Shao *et al.*, Int. J. Hydrogen Energy 38, 7070 (2013). Copyright
 2013 by Elsevier.

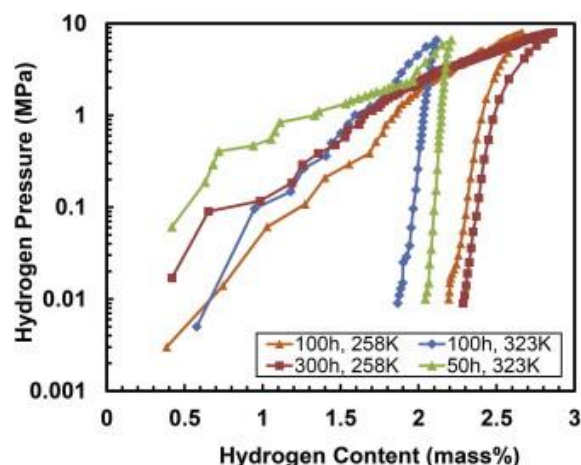


Fig. 13. PCT curves at 258 K and 323 K of the $Mg_{50}Co_{50}$ alloys milled for different durations (50 h, 100 h, and 300 h). Reproduced by permission from Shao *et al.*, Int. J. Hydrogen Energy 38, 7070 (2013). Copyright 2013 by Elsevier.

3.1.3 Doping catalytic additives

Doping catalytic additives has demonstrated as the most promising strategy to improve the reaction kinetics of Mg-H in Mg-based systems. This is mainly because the addition of catalysts can effectively reduce the reaction energy barrier, thus accelerating the hydrogen absorption/desorption rate of Mg-H systems. Several catalysts were employed such as transition metals,[126-130] metal oxides,[5, 7, 33, 131] intermetallic compounds that absorb hydrogen in milder conditions,[25, 132] and carbon materials.[133, 134]

In addition to metallic elements (discussed in section 2), some transition metal oxides, i.e., Nb_2O_5 , TiO_2 , V_2O_5 , Cr_2O_3 , Mn_2O_3 , Fe_3O_4 , CuO and SiC [33, 131] can also be added to elevate the hydrogenation and dehydrogenation performance of Mg-based alloys. For example, Nb_2O_5 proved to have more obvious enhancement in kinetics[135-

144] in comparison with other oxides. The hydrogen desorption/absorption kinetics below 5 min at 300 °C could be obtained with Nb or Nb₂O₅ addition.[144-146] Bhat *et al.*[143] reported that nanocrystalline Nb₂O₅ with high specific surface area induce the fastest kinetics than commonly used Nb₂O₅ (Figure 14). A further improvement in the sorption properties of Nb₂O₅ doped MgH₂ was found when a small amount of Cr₂O₃ was added (Figure 15) by Patah *et al.*[135] They reported a drastic reduction in the activation energy of Cr₂O₃ and Nb₂O₅ doped MgH₂ up to 136 kJ·mol⁻¹ in comparison with 197 kJ·mol⁻¹ and 206 kJ·mol⁻¹ for 1 mol% doped MgH₂ and pure MgH₂ respectively. Although the explanation for the action of these catalysts is still not clear, it is suggested that these catalysts are responsible for modification of Mg surface on mechanochemical treatment destruction of MgO layer, the formation of active nucleation centers and partial reduction of the oxides to form metal clusters (V, Nb).[147]

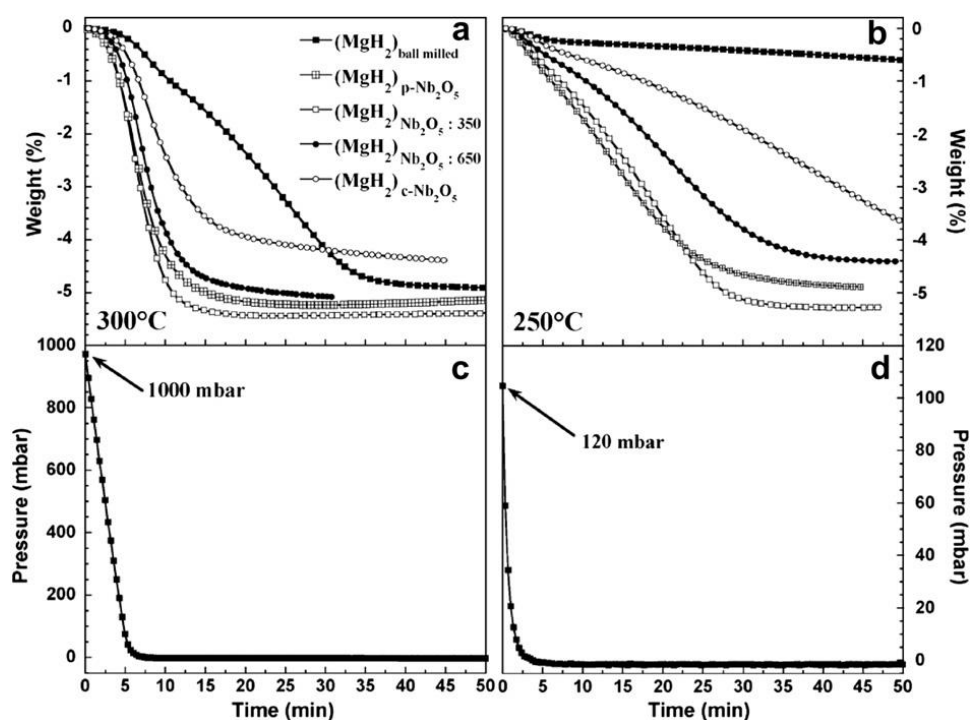


Fig. 14. Hydrogen desorption kinetics of $(\text{MgH}_2)_{\text{bm}}$ and selected $(\text{MgH}_2)_{\text{catalyst}}$ at (a) 300 °C and (b) 250 °C, and their corresponding pressure (c) and (d) during desorption, respectively. Reproduced by permission from Bhat *et al.*, J. Alloys Compd. 460, 507 (2008). Copyright 2008 by Elsevier.

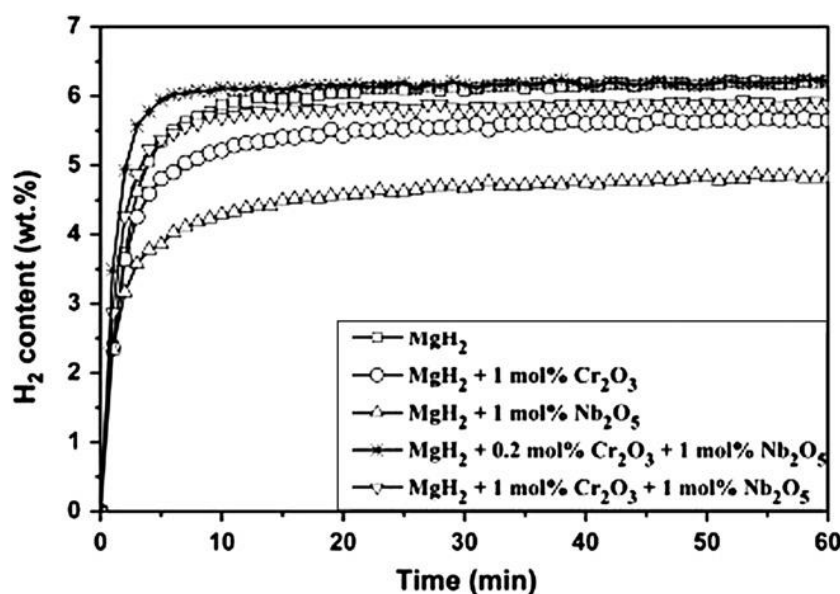


Fig. 15. The amount of the hydrogen absorbed as a function of reaction time at 300 °C under 1 MPa H_2 . Reproduced by permission from Patah *et al.*, Int. J. Hydrogen Energy 34, 3032 (2009). Copyright 2009 by Elsevier.

Wang *et al.*[148] synthesized Mg-Ni-MnO_2 by mechanical alloying and indicated that the hydrogenation of the alloy reaches 6.2 wt.% within 50 s at 200 °C under pressure of 2.0 MPa. The deposit-taking 6.2 wt.% hydrogen can be released in full within 400 s. Zou and his collaborators[149] prepared the Mg-TM-La ($\text{TM} = \text{Ti, Fe, Ni}$) ternary composites by arc plasma evaporation. The detailed investigation[150] of the hydrogen storage properties of the as-formed composites presented a remarkable modification in the hydrogenation kinetics as well as a decrease of hydrogen release

temperature, which is ascribed to the catalytic effect of Mg_2Ni and La_2O_3 .

In addition, the addition of new catalyst SiC has been reported to improve the hydrogenation properties of MgH_2 by Ranjbar *et al.* [136], e.g., the improved hydrogen absorption/desorption kinetics and increased capacity of MgH_2 caused by increasing the surface area and defect concentration. An additional improvement was achieved by adding catalyst Ni to the MgH_2/SiC composite. Halides can also enhance the hydrogenation and dehydrogenation performance of Mg-based alloys.[1, 150, 151] For example, Ismail *et al.* [152] used 10 wt.% LaCl_3 to ball mill with Mg hydride. They proved that introducing LaCl_3 to the alloys can decrease the dehydrogenation temperature by 50 °C and minimize the activation energy of hydrogen release by 23 kJ/mol, respectively, when comparing to the as-milled pure Mg hydride. The hydrogenation capacities of the doped and pure Mg hydride are respectively 5.1 wt.% and 3.8 wt.% within 2 mins at temperature of 300 °C. Meanwhile, 4.2 wt.% hydrogen can desorb from doped Mg hydride, but only 0.2 wt.% from the pure Mg hydride. Clearly, doping LaCl_3 can boost the kinetics owing to the catalytic effect of the La-Mg alloy and the MgCl_2 produced at the heating process. This study indicates that halide can encourage the refinement of metal powder of Mg-Ni alloy in the ball milling process, and effectually modulate the metal surface by destroying the oxidation layer on the metal surface, so as to promote the hydrogenation and dehydrogenation reaction of the alloy, which is particularly prominent in the first hydrogen absorption of the alloy.

Table 4. Hydrogenation properties for Mg-based alloys doping catalytic additives

Material	Temperature (°C)	Pressure conditions (bar)	Kinetics (min)	Max. Hydrogen (wt.%)	Ref.
MgH ₂ -17 wt.% Nb ₂ O ₅	T _{abs} : 274 T _{des} : 274	P _{abs} : 10 P _{des} : 0.001	t _{abs} : 2 t _{des} : 3	7.0	
Mg-10 wt.% Cr ₂ O ₃	T _{abs} : 300 T _{des} : 300	P _{abs} : 10 P _{des} : 1	t _{abs} : 3 t _{des} : 5	6.0	
MgH ₂ -1mol% La ₂ O ₃	T _{abs} : 303 T _{des} : 303			6.0	
MgH ₂ +1 mol% Cr ₂ O ₃ +0.2 mol% Nb ₂ O ₅	T _{abs} : 300		t _{abs} : 5 t _{des} : 20	6.0	
Mg-3Ni-2MnO ₂	T _{abs} : 200 T _{des} : 310	P _{abs} : 20 P _{des} : 1	t _{abs} : 50 s t _{des} : 400 s	6.2	[148]
Mg-10 wt.% LaCl ₃	T _{abs} :300		t _{abs} : 2	5.1	[152]

700 **3.1.4 Forming nanocomposite alloys**

701 Early in the 1990s, it has been reported that better comprehensive hydrogen storage
702 properties of Mg-based alloys can be achieved once combining the Mg-based hydrides
703 with other types of alloys that have excellent hydrogen kinetics. As these two
704 components can simultaneously absorb/desorb hydrogen during the
705 hydriding/dehydriding process, a cooperative interaction might be existed between
706 them to improve the hydrogen storage performances as well as the thermodynamics.
707 Thus, Mg-based hydrogen storage nanocomposite materials have been extensively
708 investigated so as to obtain hydrogen storage content up to 5 wt.% (Mg content larger
709 than 90 wt.%), under milder conditions.

710 A series of new Mg-based hydrogen storage nanocomposites have been synthesized

by the addition of LaNi₅, FeTi, C and all kinds of organic compounds, such as Mg-x wt.% LaNi₅, Mg-x wt.% FeTi, Mg-x wt.% CFMmNi₅, Mg₂Ni-x wt.% Ti₂Ni, Mg-Mg₂Ni_{0.75}Fe_{0.25}, Mg-C and tetracyanoethylene(TCNE)-Mg₂Ni, phthalonitrile(PN)-Mg₂Ni, naphthacene-Mg₂Ni and chloranil-Mg₂Ni, etc. The hydrogen storage properties of some nanocomposites are summarized in Table 5.[153, 154]

Table 5. Properties of some Mg-based nanocomposite hydrogen materials. Reproduced by permission from Broom *et al.*, Springer London (2011). Copyright 2011 by Springer-Verlag London.

Composite	Hydrogen storage capacity (wt.%)	ΔH	ΔS
		(kJ (mol ⁻¹ H ₂))	(K ⁻¹ mol ⁻¹ H ₂))
Mg-30 wt.% CFMmNi ₅ *	5.6(500 °C)	-29	-112.14
Mg-30 wt.% LaNi ₅	5.0(300 °C)	-	-
Mg-Mg ₂ Ni _{0.75} Fe _{0.25}	3.3(320 °C)	77.3(lower)	37.9
		65.2(higher)	16.2
Mg ₂ Ni-40 wt.% Ti ₂ Ni	165mAh·g ⁻¹	-	-
PN- Mg ₂ Ni	-	66.4	-
(Mg-C) _{ChorTHF}	(180 °C)	-	-
Ml _{0.7} Mg _{0.3} Ni _{3.2}	1.7(25 °C)		
LaCaMgNi ₉	1.8(20 °C)	-33.0	-120
CaTiMgNi ₉	1.87(20 °C)	-33.4	-121.0
LaCaMgNi ₆ Al ₃	1.87(20 °C)	-30.0	-101.3
LaCaMgNi ₆ Mn ₃	1.80(20 °C)	-32.3	-111.0

In addition, Zhu and his colleagues [27, 155] prepared Mg-MmM₅ (LaNi₅-based RE alloys) nanocomposites by the mechanical alloying. Particularly, the microstructures and hydrogenation properties of ball-milled Mg-MmNi_{5-x}M₅ nanocomposite systems have been studied, exhibiting the existence of nanometer-sized MmNi_{5-x}M_x-Mg and Mm₂Mg₁₇ phases and the improved hydrogen absorption properties, as shown in Figure 16. Gross *et al.*[97] then prepared La₂Mg₁₇-LaNi₅ nanocomposites via ball milling as well, showing superior kinetics to the properties of pure La₂Mg₁₇. The La₂Mg₁₇-LaNi₅ composite comprises a complicated porous mixture of three phases: Mg₂Ni (~1 μm), La (~100 nm), and Mg. During the process of hydrogenation and hydrogen release, the complex interactions between various phases, the changes in phase structures, and the synergistic effect between various phases might cooperatively to improve the kinetic performance of Mg.[156] For example, the hydrogenation and dehydrogenation kinetics of Mg in La₂Mg₁₇-LaNi₅ composites are actually catalytically boosted by closely contacting with Mg₂Ni, while slightly influenced by the La phase. In other words, the properties of hydrogen storage materials might be effectively modulated when the heterogeneous complex system (including adding catalyst phase) is achieved.

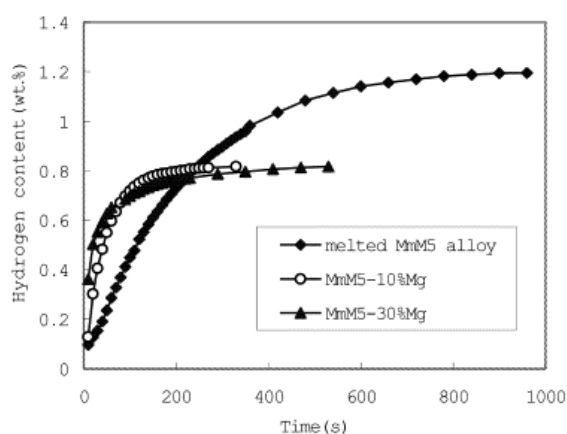


Fig. 16. Kinetic curves for melted MmM_5 alloy and nanophase composite of compositions MmM_5 -10% Mg and MmM_5 -30% Mg measured under isobaric conditions at 333 K. Reproduced by permission from Zhu *et al.*, J. Alloys Compd. 330-332, 708 (2002). Copyright 2012 by Elsevier.

AB_3 -based composites, like $LaCaMgNi_9$, $CaTiMgNi_9$, $LaCaMgNi_6Al_3$, and $LaCaMgNi_6Mn_3$ were formed via partially substituting. Interestingly, every alloy can be easily activated at ambient temperature under 3.3 MPa hydrogen pressure and the hydrogen storage of which are 1.8 wt.% hydrogen.[28, 29] Peng and his coworkers[157] proposed a $Ml_{0.7}Mg_{0.3}Ni_{3.2}$ (Ml expresses La-rich mischmetal) hydrogen storage alloy via induction melting and proved that this alloy owns a multi-phase microstructure involving $(MlMg)Ni_3$, $(MlMg)Ni_2$, and $MlNi_5$ phases, reaching a summit hydrogen storage content of 1.7wt.% at ambient temperature. Besides, they reported that the grain size apparently alters the hydrogen storage content of AB_3 -base Ml-Mg-Ni multi-phase alloys as well. More specifically, the hydrogen storage capacity declines with grain size decreasing, which is ascribed to the inadequate hydrogen storage in the grain boundary region.[157, 158]

By reactive milling, Floriano *et al.*[21] prepared Mg-based nanocomposites involving Ti-Cr-V alloys as additives for hydrogen storage. Especially, Ti-Cr-V -based alloys are one of the earliest candidates for practical hydrogen storage applications, which possess the BCC solid solution structure and can absorb up to 3.7 wt.% hydrogen at ambient temperature. The doping of TiCrV and $TiCr_{1.2}V_{0.8}$ alloys significantly enhances the dehydrogenation properties of Mg in their corresponding Mg-based nanocomposites, in comparison with their counterparts without additive. They also found that Mg-based nanocomposites containing an amount of 5 mol% of TiCrV can contribute to the optimum hydrogen storage properties, showing a more effective

reduction in desorption temperature ($\sim 240\text{ }^{\circ}\text{C}$) (than the composite containing $\text{TiCr}_{1.2}\text{V}_{0.8}$ alloy). Furthermore, faster absorption and desorption kinetics at temperatures of $275\text{ }^{\circ}\text{C}$ and $300\text{ }^{\circ}\text{C}$ can be obviously observed for the Mg-based nanocomposites containing 5 mol% of TiCrV and $\text{TiCr}_{1.2}\text{V}_{0.8}$ in comparison with the pure Mg.

The above reviewed experimental results suggest that, by forming the Mg-based nanocomposites, the additions can be inlaid on the surface of matrix particles (such as Mg or Mg_2Ni particles) and change the microstructures and phase constitutions, which might provide more active sites and pathways for hydrogen sorption and diffusion. Generally, single-phase hydrogen storage materials hardly fulfill the requirements of practical applications. Based on the advantages of each sole-phase material, it may be possible to achieve thermodynamics and kinetics dual tuning. In this regard, the incorporation of doping catalysis and nanostructuring or destabilization to establish the Mg-based nanocomposite/multiphase systems might be an effective methodology to dually tailor the thermodynamics and kinetics of Mg-based systems.

3.2 Thermodynamic modifying

Compared with the thermodynamic destabilization by solid solution,[159] alloying is more effectual to improve the thermodynamics of MgH_2 in Mg-based alloys. The added alloying metals (e.g., Si, Al, Ge) may combine with Mg to generate diverse stable phases, which are likely to alter the reaction pathway and decrease the dehydriding enthalpy further. Figure 17 schematically displays an accepted enthalpy diagram to exhibit how the additive destabilizes the tightly bound hydride.[160] The alloying element, B, decreases the hydrogen release enthalpy via the synthesis of AB_x and successfully undermines the stability of the hydride, AH_2 . Consequently, this reaction existing with a decreased enthalpy can raise the equilibrium pressure and decrease the

dehydrodring temperature.

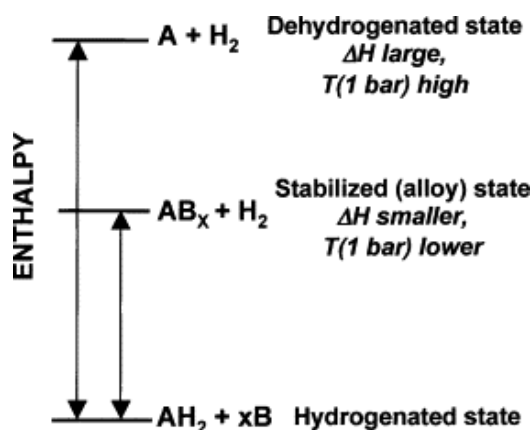


Fig. 17. Generalized enthalpy diagram illustrating destabilization through alloy formation upon dehydrogenation. Including the alloying additive, B, reduces the enthalpy for dehydrogenation through the formation of AB_x and effectively destabilizes the hydride AH_2 . Reproduced by permission from Vajo *et al.*, J. Alloys Compd. 446-447, 409 (2007). Copyright 2007 by Elsevier.

Alloying some typical elements, such as Si, Ge, Sn, and Al, etc., with Mg, have been widely investigated as well, aiming to alter thermodynamic stabilization properties of Mg-based alloys. For example, Vajo *et al.*[161]reported that alloying Mg with Si can decrease the enthalpy markedly by changing the pathway of the dehydrogenation reaction. Upon the hydrogen release of MgH_2 , Mg interacts with Si to produce a more stable compound (Mg_2Si) with the decreased dehydrogenation enthalpy.

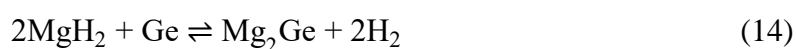
The de/hydrogenation of the MgH_2 -Si system follows the reaction mechanism as below (Eq. (13)):[85]



Alloying Si with MgH_2 is predicted to effectively undermine the Mg-H bond with a decreased enthalpy of 41 kJ ($mol^{-1} H_2$) owing to the existence of Mg_2Si .[85]

Furthermore, thermodynamic calculations indicate the release temperatures for the equilibrium pressure of 1 bar and 100 bars are approximately 293 K and 423 K, respectively. Therefore, it might suggest that the MgH₂/Si system, with a 5.0 wt.% hydrogen storage content, could be applied for hydrogen storage at low temperatures. Nevertheless, there fund a difficulty in hydrogen re-absorption of Mg₂Si resulted from the poor kinetic properties as well as the mass transport of Mg and Si into divided phases.[162, 163]

Gennari and his collaborators[164] discovered that the existence of Ge can reduce the hydrogen desorption temperature of Mg₂Ge from 323 to 423 K, which was successfully synthesized via mechanical milling. In addition, Walker *et al.*[165] accomplished the ball-milling reaction of MgH₂ with Ge under Ar atmosphere to synthesize the Mg₂Ge alloy (Eq. (14)).



Their results demonstrated that Ge can destabilize the thermodynamics of MgH₂, leading to the remarkable reduction of dehydrogenation enthalpy to 14 kJ (mol⁻¹ H₂) and temperature to 403 K. However, the dehydrogenation product Mg₂Ge cannot re-absorb hydrogen to generate MgH₂ and Ge. Meanwhile, the additional Si and Ge cannot produce their hydrides in the Mg-based alloys as well. Therefore, the hydrogen storage content is partly decreased.

Some works have also shown that the addition of Sn may play a beneficial effect on the dehydrogenation properties of Mg and Mg-based alloys. For example, the Sn/MgH₂ nanocomposite formed by mechanical milling presents a considerably decreased dehydrogenation temperature.[164] Chen *et al.*[166] discovered the presence of a weakened Mg-H bond via partial replacement of Sn for Mg by the insight into the electron structure and charge density of MgH₂,

Based on the Mg-Sn binary phase diagram,[68, 166] the equilibrium solubility of Sn in Mg can be insignificantly reduced below 573 K, meaning that it's hardly for Sn to dissolve in Mg lattice. There present two eutectic reactions containing the Mg/Mg₂Sn and Mg₂Sn/Sn mixtures. Recently, Urretavizcaya and Meyer found the possibility of shifting the cubic Mg₂Sn to the metastable hexagonal Mg₂Sn via the mechanical mixing of Mg and Sn under Ar or hydrogen atmosphere.[167] Meanwhile, Mg₂Sn might catalyze the hydrogenation/dehydrogenation of Mg due to the demonstrated mechanism resembling the eutectic mixtures of Mg/Mg₂Ni.[168] Besides, in the view of the good size figure of Mg and Sn atoms, the solubility of Sn in Mg could be further enlarged via ball milling. The synthesis of Mg(Sn) solid solution might elevate the hydrogen storage content owing to the lack of affinity of Sn to H than Mg.

Moreover, researchers proved that the solubility of Sn in Mg lattice is insignificant resulted from the Mg₂Sn formed preferentially. While the additional Sn improves the grain refinement of Mg owing to the production of Mg₂Sn. Although Mg₂Sn can hardly storage hydrogen practically, the ball-milled Mg/Mg₂Sn nanocomposites present hydrogenation/dehydrogenation kinetic properties along with destabilized thermodynamics as shown in Figure 18.[166]

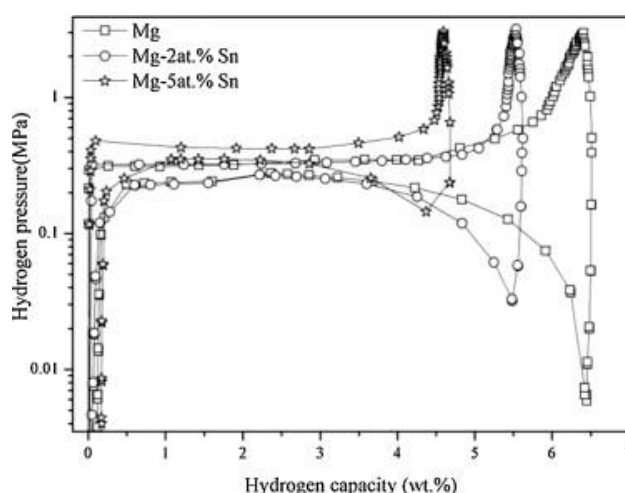
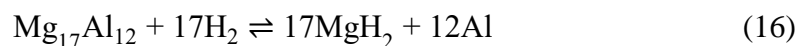


Fig. 18. PCI curves at 596K for Mg, Mg-2 at.% Sn and Mg-5at.% Sn. Reproduced by permission from Zhong *et al.*, J. Alloys Compd. 509, 4268 (2011). Copyright 2011 by Elsevier.

Zaluska and his colleagues[18] proved that combining Mg with Al might destabilize the MgH₂ in thermodynamics. In 1978, Douglass[67] obtained 6.3 wt.% hydrogen storage capacity by melting Mg-Al alloy. The hydrogen storage performance of some types of Mg-Al alloys with different compositions, such as Mg₃Al₁₂(γ), Mg₁₇Al₁₂(γ), and Mg₂Al₃(β), and the effect of adding the third element on its hydrogen storage properties are summarized in Figure 6.[45, 69] The problem is that the Mg-Al alloy will undergo disproportionation reaction at a higher temperature (348 °C) to generate MgH₂ and Al according to the reaction (Eq. (15-16)):



The reaction rate of Mg-Al alloys, however, seems to be sluggish, thus leaving the infeasible application for this system. The theoretical hydrogen capacity of MgH₂-Al is up to 4.4 wt.% and the dehydrogenation enthalpy reduces slightly by 6 kJ (mol⁻¹ H₂). But the destabilization effect of this system is relatively weak (only around 50 K reduction in decomposition starting temperature).[169] Especially, the reversible hydrogen absorption was achieved through three transformation steps, from the initial reaction from only Mg to form MgH₂, then the decomposition of the γ-Mg₁₇Al₁₂ phase into the Mg-poor β-Mg₂Al₃ phase, and the final formation of the Mg-hydride phase from the resulting Mg₂Al₃. [170]

Besides, Mg-based ternary alloys, such as Mg-Al-Me, Mg-Al-Ti, Mg-Fe-Ti and Mg-Al-Fe, have also been investigated. For example, Kalisvaart *et al.* [171] focused on

hydrogen sorption properties of 1.5 mm thick Mg-based films with Al, Fe, and Ti as alloying elements. These ternary alloys display remarkable sorption behavior, e.g., the films can absorb 4-6 wt.% hydrogen in seconds and desorbing in minutes at 200 °C. Meanwhile, this sorption kinetics are stable for the Mg-Al-Ti and Mg-Fe-Ti alloys, which showed no degradation in capacity even after 100 absorption/desorption cycles. For the Mg-Al-Fe alloy, the properties are clearly worse compared to the other ternary counterparts.

Table 6. Hydriding characteristics of various binary and ternary Mg-Al alloys.

Alloy composition (atomic ratio)	δT^* (°C)	Hydrogen absorbed (wt.%)	Plateau pressure at 300°C (atm)
Mg ₁₇ Al ₁₂ (γ -phase)	-	3.31	-
Mg ₄ Al ₅ (ϵ -phase)	-	2.77	-
Mg ₂ Al ₃ (β -phase)	-	3.28	-
MgAl (β + γ -phase)	-	0.38	-
Mg _{0.62} Al _{0.38}	19	2.30	1.4
Mg _{0.59} Al _{0.36} Ni _{0.05}	28	3.36	1.8
Mg _{0.59} Al _{0.36} La _{0.05}	31	3.04	1.9
Mg _{0.59} Al _{0.36} Y _{0.05}	30	2.01	2.2
Mg _{0.56} Al _{0.34} La _{0.10}	-	2.12	1.7
Mg _{0.56} Al _{0.34} Y _{0.10}	40	3.29	2.1-2.6
Mg _{0.56} Al _{0.34} Ni _{0.05} Y _{0.05}	-	2.58	1.5
Mg _{0.56} Al _{0.34} Mm _{0.10} [†]	-	2.15	1.8
Mg _{0.80} Al _{0.10} Y _{0.10}	65	4.08	1.7

Mg _{0.80} Al _{0.10} La _{0.10}	123	4.22	2.1
Mg _{0.91} Al _{0.09}	-	7.0	-
Mg _{0.9} Al _{0.1}		H/M=1.75	
(Mg ₇₀ Al ₃₀)-99+(Nb ₂ O ₅)-1mol.%		4.7(250 °C)	
Mg ₇₀ Al ₁₅ Ti ₁₅		4.0	-
Mg ₈₅ Al _{7.5} Ti _{7.5}		5.4	

* The temperature rise observed during hydriding which is found to be a good qualitative measure of hydriding kinetics. The increase in the δT value indicates relatively the rapidity of hydriding kinetics.

† Mm = Mischmetal

3.3 Kinetic and thermodynamic dual modifying

3.3.1 Tuning alloy composition

In recent works, it has been found that some specific Mg-based hydrogen storage alloys are able to realize the dual tuning effects on the thermodynamic and kinetic properties. Normally, the catalytic elements/alloys should be added to these dual modifying-effect Mg-based alloys for further optimization, such as most widely investigated Mg (In)-based alloys.

For example, Zhou *et al.*[172] used Ti intermetallic compound to promote the dehydrogenation kinetic properties of Mg(In) solid solution. They reported that the destabilization in thermodynamics of Mg_{0.1}In alloy can also possess excellent hydrogen desorption kinetics, e.g., it begins to release hydrogen at about 100 °C and hydrogen can be completely released at 150 °C after 3 hours,[173] simultaneously destabilizing the thermodynamics and kinetics of MgH₂. However, the formation of Mg(In) solid

solution demands the association of prolonging sintering and mechanically milling, ascribing to the greatly varied atomic radii between the soft metal In (1.93 Å) and Mg (1.73 Å),[87] which might lead to rather sluggish dehydriding kinetics of this alloys. Ouyang *et al.*[174] subsequently developed an innovative efficient approach, plasma milling, to synthesize the Mg(In)-MgF₂ composite that shows the enhanced dual modifying effects. The hydrogen capacity of Mg(In) solid solution in Mg(In)-MgF₂ composite is improved significantly up to 5.16 wt.%, as shown in Figure 20. Simultaneously, the kinetics is also boosted due to the catalysis *in situ* formed MgF₂. In this connection, the *in situ* formed MgF₂ serves as a catalyst to accelerate the reaction rate of the following equation:

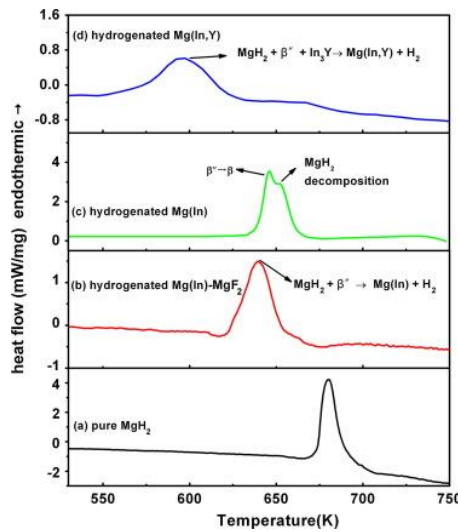
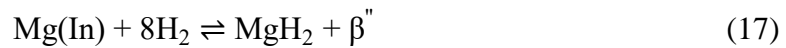


Fig. 19. DSC curves for (a) Pure MgH₂, (b) hydrogenated Mg(In)-MgF₂ composite, (c) hydrogenated Mg(In) solid solution and (d) hydrogenated Mg(In, Y) solid solution, with a heating rate of 2 K/min. Reproduced by permission from Ouyang *et al.*, J. Alloys Compd. 586, 113 (2014). Copyright 2014 by Elsevier.

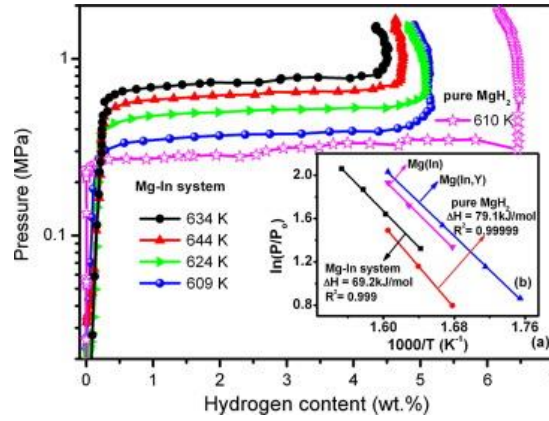


Fig. 20. (a) PCI curves for the hydrogen desorption of the Mg(In)-MgF₂ composite and pure MgH₂, (b) Van't Hoff plots of the Mg(In)-MgF₂ composite, pure MgH₂, Mg(In) and Mg(In, Y) solid solutions. Reproduced by permission from Ouyang *et al.*, J. Alloys Compd. 586, 113 (2014). Copyright 2014 by Elsevier.

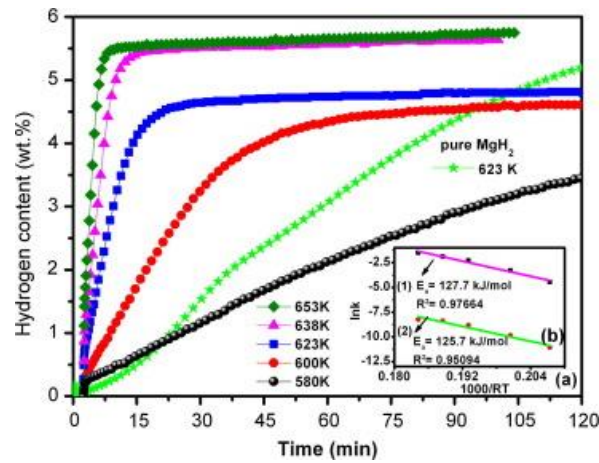
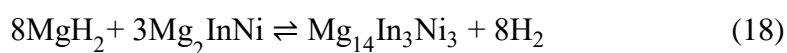


Fig. 21. (a) Dehydrodring kinetic curves for the hydrogenated Mg(In)-MgF₂ composite, (b): (1) and (2) are the Arrhenius plots fitted by the JMAK model and the Jander diffusion model, respectively. Reproduced by permission from Ouyang *et al.*, J. Alloys Compd. 586, 113 (2014). Copyright 2014 by Elsevier.

Meanwhile, Cao *et al.*[175] synthesized Mg₉₈In₅Al₅Ti alloy by plasma milling to explore the dual-modifying effects of added elements of In, Al, and Ti. In particular,

Lu *et al.*[176, 177] described the hydrogen storage performance of a set of Mg-In-Ni ternary alloys and their structural transformation during hydrogenation and dehydrogenation, and investigated the mechanisms of dual modifying effects. For the first time, they observed the reversible hydrogen-induced phase change between the two new Mg-In-Ni ternary intermetallic compounds ($\text{Mg}_{14}\text{In}_3\text{Ni}_3$ and Mg_2InNi). In the hydrogenation process, the $\text{Mg}_{14}\text{In}_3\text{Ni}_3$ alloy breaks up into a combination of MgH_2 and Mg_2InNi , which is entirely reversible in the dehydrogenation reaction with a hydrogen storage content of 1.8 wt.% (Eq. (18)).



The reaction enthalpy and dehydrogenation activation energy for the dehydrogenation of MgH_2 and Mg_2InNi were calculated to be $70.1 \text{ kJ mol}^{-1} \text{ H}_2$ and 78.5 kJ mol^{-1} , respectively, both of which are lower than that of pure MgH_2 (Figure 22). The *in-situ* XRD patterns for the hydrogen release of hydrogen absorbed $\text{Mg}_{14}\text{In}_3\text{Ni}_3$ at several temperatures are displayed in Figure 23. The reversible synthesis of these two novel Mg-In-Ni ternary phases destabilizes both the dehydrogenation thermodynamics and kinetics of MgH_2 .

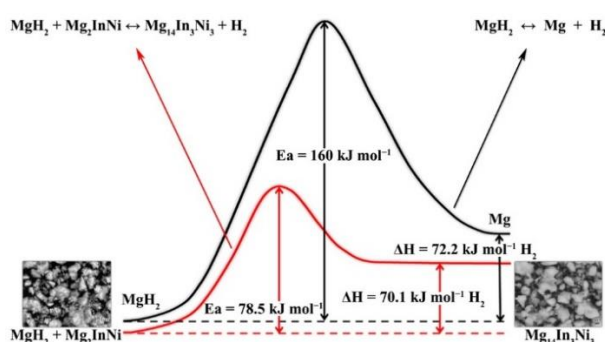
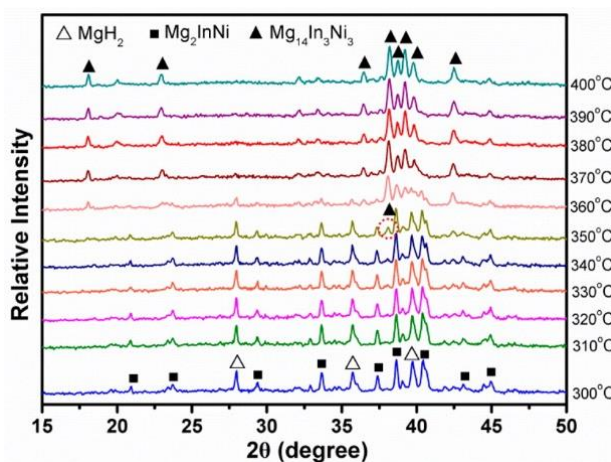


Fig. 22. The energy barrier schematic diagram of Mg-In-Ni ternary alloys. Reproduced by permission from Lu *et al.*, J. Phys. Chem. C 119, 26858 (2015). Copyright 2015 by



945

946 Fig. 23. *In situ* XRD patterns for the dehydrogenation of hydrogenated $\text{Mg}_{14}\text{In}_3\text{Ni}_3$ (the
 947 mixture of MgH_2 and Mg_2InNi) at different temperatures. Reproduced by permission
 948 from Lu *et al.*, J. Phys. Chem. C 119, 26858 (2015). Copyright 2015 by ACS
 949 publications.

950 3.3.2 Adopting novel synthetic techniques

951 Thus far, many new techniques have been developed to synthesize MgH_2 for
 952 hydrogen storage, such as mechanical milling,[178] thin-film technology,[179]
 953 hydrogen plasma metal reaction,[180] hydriding chemical vapor deposition,[9] melt
 954 spinning,[181] severe plastic deformation,[182, 183] chemical reduction,[184] and
 955 electro-chemical deposition.[185] Particularly, severe plastic deformation technique
 956 has been receiving extensive attention as it can be developed to control the
 957 microstructural evolution (decreasing grain sizes, increasing the density of defects,
 958 inducing the formation of textures, designing special types of grain boundaries and
 959 increase the degree of supersaturation), control the surface reactivity (and easy
 960 contamination that comes with it) and evaluate alternatives for scaling-up production.
 961 [183, 186] For example, Mg and MgH_2 powders have been processed by high-pressure

torsion (HPT) to reduce the crystallite size, generate defects and promote consolidation of the powders, which clearly improve the surface resistance to atmospheric gases.[183] With the same principle, there are many types of severe plastic deformation techniques, e.g., HPT,[112, 187] extensive equal-channel angular pressing (ECAP) [188], and accumulative roll bonding (ARB), etc.[189, 190]

Skripnyuk *et al.*[182] was pioneered to fabricate the nanostructured ZK60 Mg-based alloys or composites by severe plastic deformation techniques. Other Mg-based alloys such as MgMnNi[191] and MgNi alloys, have also been processed by severe plastic deformation techniques later,[192] e.g., showing the improvement in hydrogenation performance of MgNi alloy associated with the chemical inhomogeneity induced by ECAP processing. Other processing technique such as extensive rolling or ARB have also been used to prepare laminate composites.[193-196] During the ARB processing, two plate specimens (different compositions or not) are stacked and rolled for several passes, as schematically shown in Figure 24, which therefore induce the severe plastic deformation with high strain and strain rate on the specimens, thereby leading to an ultra-fine microstructure finally.

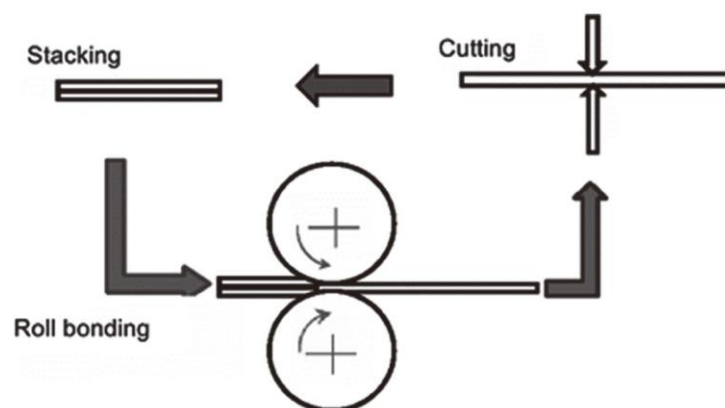


Fig. 24. Schema of ARB process. Reproduced by permission from Valiev *et al.*, Prog. Mater Sci. 51, 881 (2006). Copyright 2006 by Elsevier

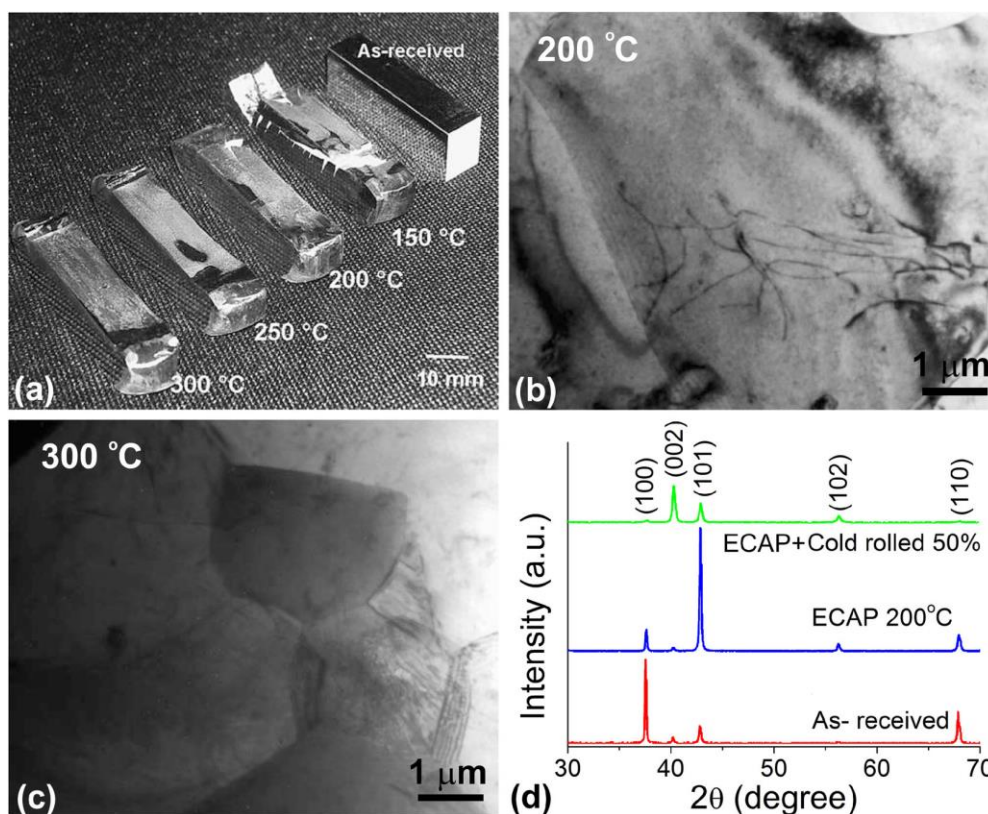


Fig. 25. AZ31 alloy processed by ECAP and ECAP plus cold rolling. (a) Photograph of the specimens after two passes of ECAP at the indicated temperatures; (b) and (c) TEM bright-field images after ECAP processing: (b) ECAP at 200°C; (c) ECAP at 300°. (d) XRD patterns comparing the conditions of as-received (extruded), after ECAP at 200°C, and after ECAP at 200 °C followed by cold rolling. Reproduced by permission from Leiva *et al.*, Int. J. Mater. Res. 100, 1739 (2009). Copyright 2009 by Carl Hanser Verlag.

In addition, different severe plastic deformation technologies have also been incorporated to modify the hydrogen storage properties of Mg-based alloys.[197] For example, Figure 25 shows the AZ31 alloy processed by ECAP and cold rolling, [198] i.e., (a) the ECAPed processed samples and in (b) and (c) the resulting microstructures after processing at 200°C and 300°C, respectively. In Figure 25(d), the XRD patterns show the effect of cold rolling in establishing the (002) texture. Huot *et al.*[199]

reviewed the use of ECAP and CR for the enhancement of hydrogen sorption properties of Mg and Mg alloys. The effects of the processing route and type of texture they produced were associated with the hydrogen storage properties. Botta *et al.*[200] also reported the positive effects of texture, small grain size and free surfaces (or interfaces) for the hydrogen storage properties, after processing commercial Mg by melt-spinning, HPT and CR.

4. Conclusion and prospects

In this review, we first introduce the classification of the Mg-based hydrogen storage alloys and then summarize some effective measures and the associated progress to enhance the hydrogen storage kinetics and thermodynamics of Mg-based compounds, such as alloying, nanostructuring, synthesizing metastable phases, doping catalytic additives, forming nanocomposite, changing the reaction way, and realizing dual modifying effects, etc. However, it should be noted that no candidate and advanced method can completely meet the demands for practical applications. For example, alloying, doping, synthesizing metastable phases, and changing the reaction path can effectively reduce the formation enthalpy; but unfortunately, sacrifice hydrogen storage content and some of the reactions are irreversible. Nanostructuring is also a promising method to modify the hydrogen storage properties, but the fabrication and weak stability of nanostructures continue to demand improvement. Forming Mg-based nanocomposite materials might be able to combine the excellence of alloy engineering, nanostructuring, and synergistic effects obtained by the RMM (reactive mechanical milling), leading to an instability in the thermodynamics of Mg/MgH₂. Therefore, further studies on the kinetics and thermodynamics of Mg-based hydrogen storage compounds are still needed to be improved to achieve the practical application goals, possibly focusing on following several aspects:

1) Increasing more characteristic octahedral and/or tetrahedral sites to contain hydrogen and additionally possible vacancies to improve the hydrogenation properties of Mg-based materials, such as amorphization via the combination of crystalline and amorphous materials.[95, 201, 202]

2) Discovering a superior strategy to maintain the structural stability of nanostructuring. Prospectively, nanostructuring can significantly lighten kinetic barriers and decrease thermodynamic stability. Nevertheless, a great challenge of stability, for example, severe aggregation and structural collapse, is still existed during the hydrogenation/dehydrogenation process. Thus, more fabrications of stabilization should be investigated to elevate the storage capacity meanwhile exploring possible stabilization for the nanosized Mg in the absence of scaffolds, such as introducing graphene nanoribbons,[203] a second phase,[18, 204] and core-shell methods,[129, 205-207], etc.

3) Developing the novel preparation techniques to realize the dual modifying of thermodynamic and kinetic properties of Mg-based alloys, such as mechanical milling for nanostructuring, doping catalytic additives, and forming nanocomposites,[178] physical/chemical deposition for realizing nanocomposites,[184] and nanostructuring by wet chemical routes [85], severe plastic deformation,[183] and electrochemical approaches.[185]

Acknowledgments

This work was supported by the National Key R&D Program of China (No. 2019YFB1505101 and 2018YFB1502101), the Foundation for Innovative Research Groups of the National Natural Science Foundation of China (No. NSFC51621001), National Natural Science Foundation of China Projects (Nos. 51771075 and 51971187) and by the Project Supported by Natural Science Foundation of Guangdong Province

of China (2016A030312011).

References

- [1] Y.H. Sun, C.Q. Shen, Q.W. Lai, W. Liu, D.W. Wang, K.F. Aguey Zinsou, Tailoring magnesium based materials for hydrogen storage through synthesis: current state of the art, *Energy Storage Materials*, 10 (2018) 168-198.
- [2] R. Mohtadi, S.I. Orimo, The renaissance of hydrides as energy materials, *Nat. Rev. Mater*, 2 (2017).
- [3] S.I. Orimo, Y. Nakamori, J.R. Eliseo, A. Züttel, C.M. Jensen, Complex hydrides for hydrogen storage, *Chem. Rev.*, 107 (2007) 4111-4132.
- [4] L. Schlapbach, A. Züttel, Hydrogen-storage materials for mobile applications, *Nature*, 414 (2001) 353-358.
- [5] K.F. Aguey Zinsou, J.R. Ares Fernandez, Hydrogen in magnesium: New perspectives toward functional stores, *Energ Environ Sci*, 3 (2010) 526-543.
- [6] A. Züttel, Materials for Hydrogen Storage, *Mater. Today*, 6 (2003) 24-33.
- [7] J.D. Li, B. Li, H.Y. Shao, W. Li, H.J. Lin, Catalysis and downsizing in Mg-based hydrogen storage materials, *Catalysts*, 8 (2018).
- [8] B. Li, J.D. Li, H.Y. Shao, L.Q. He, Mg-based hydrogen absorbing materials for thermal energy storage-a review, *Appl. Sci.*, 8 (2018).
- [9] H.Y. Shao, G.B. Xin, J. Zheng, X.G. Li, E. Akiba, Nanotechnology in Mg-based materials for hydrogen storage, *Nano Energy*, 1 (2012) 590-601.
- [10] D.L. Zhao, Y.H. Zhang, Research progress in Mg-based hydrogen storage alloys, *Rare Met.*, 33 (2014) 499-510.
- [11] N. Cui, P. He, J.L. Luo, Magnesium-based hydrogen storage materials modified by mechanical alloying, *Acta Mater.*, 47 (1999) 3737-3743.
- [12] J.L. Bobet, E. Akiba, Y. Nakamura, B. Darriet, Study of Mg-M (M = Co, Ni and Fe) mixture elaborated by reactive mechanical alloying-hydrogen sorption properties, *Int. J. Hydrogen Energy*, 25 (2000) 987-996.
- [13] S.I. Yamaura, H.Y. Kim, H. Kimura, A. Inoue, Y. Arata, Electrode properties of rapidly solidified $Mg_{67}Ni_{23}Pd_{10}$ amorphous alloy., *J. Alloys Compd.*, 347 (2002) 239-243.
- [14] Z. Dehouche, R. Djaozandry, J. Goyette, T.K. Bose, Evaluation techniques of cycling effect on thermodynamic and crystal structure properties of Mg_2Ni alloy, *J. Alloys Compd.*, 288 (1999) 269-276.
- [15] W.Y. Li, C.S. Li, H. Ma, J. Chen, Magnesium nanowires: Enhanced kinetics for hydrogen absorption and desorption, *J. Am. Chem. Soc.*, 129 (2007) 6710-6711.
- [16] T.K. Nielsen, K. Manickam, M. Hirscher, F. Besenbacher, T.R. Jensen, Confinement of MgH_2 Nanoclusters within Nanoporous Aerogel Scaffold Materials, *Acs Nano*, 3 (2009) 3521-3528.
- [17] Z. Zhao Karger, J.J. Hu, A. Roth, D. Wang, C. Kubel, W. Lohstroh, M. Fichtner, Altered thermodynamic and kinetic properties of MgH_2 infiltrated in microporous scaffold, *Chem. Commun.*, 46 (2010) 8353-8355.
- [18] A. Zaluska, L. Zaluski, J.O. Ström-Olsen, Structure, catalysis and atomic reactions on the nano-scale: a systematic approach to metal hydrides for hydrogen storage, *Appl. Phys. A*, 72 (2001) 157-165.
- [19] J.G. Zhang, Y.F. Zhu, H.J. Lin, Y.N. Liu, Y. Zhang, S.Y. Li, Z.L. Ma, L.Q. Li, Metal hydride nanoparticles with ultrahigh structural stability and hydrogen storage activity derived from microencapsulated nanoconfinement, *Adv. Mater.*, 29 (2017) 1700760.
- [20] J. Cui, L.Z. Ouyang, H. Wang, X.D. Yao, M. Zhu, On the hydrogen desorption entropy change of

modified MgH_2 , *J. Alloys Compd.*, 737 (2018) 427-432.

[21] R. Floriano, D.R. Leiva, J.G. Dessi, A.A.C. Asselli, A.M. Jorge, W.J. Botta, Mg-based nanocomposites for hydrogen storage Containing Ti-Cr-V alloys as additives, *Mat. Res.*, 19 (2016) 80-85.

[22] Y. Wang, Q.Y. Lu, N. Peng, F.M. Xiao, R.H. Tang, Effect of heat-treatment process on properties of rare earth Mg-based system hydrogen storage alloys with AB_3 -type, *J. Rare Earths*, 24 (2006) 340-342.

[23] M. Zhu, H. Wang, L.Z. Ouyang, M.Q. Zeng, Composite structure and hydrogen storage properties in Mg-base alloys, *Int. J. Hydrogen Energy*, 31 (2006) 251-257.

[24] D. Cracco, A. Percheron-Guegan, Morphology and hydrogen absorption properties of an AB_2 type alloy ball milled with Mg_2Ni , *J. Alloys Compd.*, 268 (1998) 248-255.

[25] G. Liang, S. Boily, J. Huot, R.J. Schulz, Hydrogen absorption properties of a mechanically milled Mg-50 wt.% LaNi_5 composite, *J. Alloys Compd.*, 268 (1998) 302-307.

[26] D. Sun, H. Enoki, M. Bououdina, E. Akiba, Phase components and hydriding properties of the sintered Mg-x wt.% LaNi_x ($x = 20-50$) composites, *J. Alloys Compd.*, 282 (1999) 252-257.

[27] M. Zhu, W.H. Zhu, C.Y. Chung, Z.X. Li, Microstructure and hydrogen absorption properties of nano-phase composite prepared by mechanical alloying of $\text{MmNi}_{5-x}(\text{CoAlMn})_x$ and Mg, *J. Alloys Compd.*, 293-295 (1999) 531-535.

[28] J. Chen, N. Kuriyama, H.T. Takeshita, H. Tanaka, T. Sakai, M. Haruta, Hydrogen storage alloys with PuNi_3 -type structure as metal hydride electrodes, *Electrochem. Solid-State Lett.*, 3 (2000) 249-252.

[29] J. Chen, H.T. Takeshita, H. Tanaka, N. Kuriyama, T. Sakai, I. Uehara, M. Haruta, Hydriding properties of LaNi_3 and CaNi_3 and their substitutes with PuNi_3 -type structure, *J. Alloys Compd.*, 302 (2000) 304-313.

[30] B. Bogdanović, B. Spliethoff, Active MgH_2 -Mg systems for hydrogen storage, *Int. J. Hydrogen Energy*, 12 (1987) 863-873.

[31] C. Zhou, H. Wang, L.Z. Ouyang, M. Zhu, The state of the art of hydrogen storage materials for high-pressure hybrid hydrogen vessel, *Materials Reports*, 33 (2019) 117-126.

[32] M. Dornheim, S. Doppiu, G. Barkhordarian, U. Boesenberg, T. Klassen, O. Gutfleisch, R. Bormann, Hydrogen storage in magnesium-based hydrides and hydride composites, *Scr. Mater.*, 56 (2007) 841-846.

[33] I.P. Jain, C. Lal, A. Jain, Hydrogen storage in Mg: a most promising material, *Int. J. Hydrogen Energy*, 35 (2010) 5133-5144.

[34] J.J. Reilly, R.H. Wiswall, Reaction of hydrogen with alloys of magnesium and nickel and the formation of Mg_2NiH_4 , *Inorg. Chem.*, 7 (1968) 2254-2256.

[35] M. Zhu, Y.S. Lu, L.Z. Ouyang, H. Wang, Thermodynamic tuning of Mg-based hydrogen storage alloys: a review, *Materials (Basel)*, 6 (2013) 4654-4674.

[36] L.J. Huang, G.Y. Liang, Z.B. Sun, Y.F. Zhou, Nanocrystallization and hydriding properties of amorphous melt-spun $\text{Mg}_{65}\text{Cu}_{25}\text{Nd}_{10}$ alloy, *J. Alloys Compd.*, 432 (2007) 172-176.

[37] A. Gebert, B. Khorkounov, U. Wolff, C. Mickel, M. Uhlemann, L. Schultz, Stability of rapidly quenched and hydrogenated Mg-Ni-Y and Mg-Cu-Y alloys in extreme alkaline medium, *J. Alloys Compd.*, 419 (2006) 319-327.

[38] T. Spassov, V. Rangelova, N. Neykov, Nanocrystallization and hydrogen storage in rapidly

1133 solidified Mg-Ni-RE alloys, *J. Alloys Compd.*, 334 (2002) 219-223.

1134 [39] K. Tanaka, Y. Kanda, M. Furuhashi, K. Saito, K. Kuroda, Improvement of hydrogen storage
1135 properties of melt-spun Mg-Ni-RE alloys by nanocrystallization, *J. Alloys Compd.*, 293-295 (1999).

1136 [40] X. Yao, G.Q. Lu, L. Li, Multi-component catalysts enhanced hydrogen storage in novel
1137 magnesium-based nanocomposites, *J. Alloys Compd.*, 2007903489 (2007).

1138 [41] X.D. Yao, G.Q. Lu, Magnesium-based materials for hydrogen storage: Recent advances and future
1139 perspectives, *Chin. Sci. Bull.*, 53 (2008) 2421-2431.

1140 [42] L.Z. Ouyang, Z.J. Cao, H. Wang, J.W. Liu, D.L. Sun, Q.A. Zhang, M. Zhu, Dual-tuning effect of
1141 In on the thermodynamic and kinetic properties of Mg_2Ni dehydrogenation, *Int. J. Hydrogen Energy*,
1142 38 (2013) 8881-8887.

1143 [43] S. Orimo, H. Fujii, Materials science of Mg-Ni-based new hydrides, *Appl. Phys. A*, 72 (2001) 167-
1144 186.

1145 [44] S.S.S. Raman, D.J. Davidson, J.L. Bobet, O.N. Srivastava, Investigations on the synthesis,
1146 structural and microstructural characterizations of Mg-based K_2PtCl_6 type (Mg_2FeH_6) hydrogen
1147 storage material prepared by mechanical alloying, *J. Alloys Compd.*, 333 (2002) 282-290.

1148 [45] P. Selvam, B. Viswanathan, C.S. Swamy, V. Srinivasan, Magnesium and magnesium alloy hydride,
1149 *Int. J. Hydrogen Energy*, 11 (1986) 169-192.

1150 [46] K. Batalovic, J. Radakovic, J. Belosevic-Cavor, V. Koteski, Transition metal doping of Mg_2FeH_6 -a
1151 DFT insight into synthesis and electronic structure, *Phys. Chem. Chem. Phys.*, 16 (2014) 12356-12361.

1152 [47] Y.J. Wang, T. Aizawa, C. Nishimura, Solid-state synthesis of hydrogen storage Mg_2Co alloys via
1153 bulk mechanical alloying, *Mater. Trans.*, 47 (2006) 1052-1057.

1154 [48] M. Polanski, T.K. Nielsen, Y. Cerenius, J. Bystrzycki, T.R. Jensen, Synthesis and decomposition
1155 mechanisms of Mg_2FeH_6 studied by in-situ synchrotron X-ray diffraction and high-pressure DSC, *Int.*
1156 *J. Hydrogen Energy*, 35 (2010) 3578-3582.

1157 [49] J. Zhang, F. Cuevas, W. Zaïdi, J.-P. Bonnet, L. Aymard, J.-L. Bobet, M. Latroche, Highlighting of
1158 a single reaction path during reactive ball milling of Mg and TM by quantitative H_2 gas sorption
1159 analysis to form ternary complex hydrides (TM = Fe, Co, Ni), *J. Phys. Chem. C*, 115 (2011) 4971-
1160 4979.

1161 [50] K.H.J. Buschow, Magnetic properties of rare earth-magnesium compounds (RMg_3), *J. Less*
1162 *Common Met*, 44 (1976) 301-306.

1163 [51] A. Kamegawa, Y. Goto, H. Kakuta, H. Takamura, M. Okada, High-pressure synthesis of novel
1164 hydrides in Mg-RE-H systems (RE = Y, La, Ce, Pr, Sm, Gd, Tb, Dy), *J. Alloys Compd.*, 408-412
1165 (2006) 284-287.

1166 [52] L.Z. Ouyang, F.X. Qin, M. Zhu, The hydrogen storage behavior of Mg_3La and $\text{Mg}_3\text{LaNi}_{0.1}$, *Scr.*
1167 *Mater.*, 55 (2006) 1075-1078.

1168 [53] L.Z. Ouyang, X.S. Yang, H.W. Dong, M. Zhu, Structure and hydrogen storage properties of Mg_3Pr
1169 and $\text{Mg}_3\text{PrNi}_{0.1}$ alloys, *Scr. Mater.*, 61 (2009) 339-342.

1170 [54] Y.Q. Tong, L.Z. Ouyang, M. Zhu, Effect of Ni on Mg based hydrogen storage alloy Mg_3Nd , *Rare*
1171 *Met.*, 25 (2006) 289-294.

1172 [55] L.Z. Ouyang, H.W. Dong, C.H. Peng, L.X. Sun, M. Zhu, A new type of Mg-based metal hydride
1173 with promising hydrogen, *Int. J. Hydrogen Energy*, 32 (2007) 3929-3935.

1174 [56] L.Z. Ouyang, L. Yao, X.S. Yang, L.Q. Li, M. Zhu, The effects of Co and Ni addition on the
1175 hydrogen storage properties of Mg_3Mm , *Int. J. Hydrogen Energy*, 35 (2010) 8275-8280.

1176 [57] L.Z. Ouyang, H.W. Dong, M. Zhu, Mg_3Mm compound based hydrogen storage materials, *J.*

Alloys Compd., 446 (2007) 124-128.

[58] H.J. Lin, L.Z. Ouyang, H. Wang, J.W. Liu, M. Zhu, Phase transition and hydrogen storage properties of melt-spun $\text{Mg}_3\text{LaNi}_{0.1}$ alloy, *Int. J. Hydrogen Energy*, 37 (2012) 1145-1150.

[59] H.Y. Shao, K. Asano, H. Enoki, E. Akiba, Preparation and hydrogen storage properties of nanostructured Mg-Ni BCC alloys, *J. Alloys Compd.*, 477 (2009) 301-306.

[60] H.Y. Shao, K. Asano, H. Enoki, E. Akiba, Preparation and hydrogen storage properties of Mg-Ni-B BCC alloys, *Mater. Sci. Forum*, 561-565 (2007) 1625-1628.

[61] C. Zhang, H. Wang, L.Z. Ouyang, H.J. Lin, M. Zhu, Effect of Cu on dehydrogenation and thermal stability of amorphous Mg-Ce-Ni-Cu alloys, *Progress in Natural Science: Materials International*, 27 (2017) 622-626.

[62] M. Hansen, K. Anderko, *Constitution of binary alloys*, McGraw-Hill, (1958).

[63] J.J. Reilly, R.H. Wiswall, The reaction of hydrogen with alloys of magnesium and copper, *Inorg. Chem.*, 6 (1967) 2220-2223.

[64] H.Y. Shao, G.B. Xin, X.G. Li, E. Akiba, Thermodynamic Property Study of Nanostructured Mg-H, Mg-Ni-H, and Mg-Cu-H Systems by High Pressure DSC Method, *J Nanomater.* (2013).

[65] F.H. Ellinger, J. C. E. Holley, B.B. Mcinteer, The Preparation and Some Properties of Magnesium Hydride, *J. Am. Chem. Soc.*, 77 (1955) 2647-2648.

[66] J. J. F. Stampfer, J. C. E. Holley, J.F. Suttle, The Magnesium-hydrogen system, *J. Am. Chem. Soc.*, (1960) 3504.

[67] D.L. Douglass, The storage and release of hydrogen from magnesium alloy hydrides for vehicular applications, *Hydrides for Energy Storage*, (1978) 151-184.

[68] R. Wiswall, Hydrogen storage in metals, *Hydrogen in metals II: Application-oriented properties*, 29 (1978) 201-242.

[69] A.F. Palacios-Lazcano, J.L. Luna-Sanchez, J. Jimenez-Gallegos, F. Cruz-Gandarilla, J.G. Cabanas-Moreno, Hydrogen storage in nanostructured Mg-base alloys, *J. Nano Res.*, 5 (2009) 213-221.

[70] L.Z. Ouyang, Z.J. Cao, L. Yao, H. Wang, J.W. Liu, M. Zhu, Comparative investigation on the hydrogenation/dehydrogenation characteristics and hydrogen storage properties of Mg_3Ag and Mg_3Y , *Int. J. Hydrogen Energy*, 39 (2014) 13616-13621.

[71] T.Z. Si, Y. Cao, Q.G. Zhang, D.L. Sun, L.Z. Ouyang, M. Zhu, Enhanced hydrogen storage properties of a Mg-Ag alloy with solid dissolution of indium: a comparative study, *J. Mater. Chem. A*, 3 (2015) 8581-8589.

[72] Y.S. Lu, H. Wang, J.W. Liu, Z.M. Li, L.Z. Ouyang, M. Zhu, Hydrogen-Induced Reversible Phase Transformations and Hydrogen Storage Properties of Mg-Ag-Al Ternary Alloys, *J. Phys. Chem. C*, 120 (2016) 27117-27127.

[73] Y.S. Lu, H. Wang, J.W. Liu, L.Z. Ouyang, M. Zhu, Destabilizing the dehydriding thermodynamics of MgH_2 by reversible intermetallics formation in Mg-Ag-Zn ternary alloys, *J. Power Sources*, 396 (2018) 796-802.

[74] M. Bhihi, M. Lakhal, S. Naji, First principle calculations for improving desorption temperature in $\text{Mg}_{16}\text{H}_{32}$ doped with Ca, Sr and Ba elements, *Bull. Mater. Sci.*, 37 (2014) 1731-1736.

[75] X. Ren, C.R. Li, Z.M. Du, C.P. Guo, S.C. Chen, Thermodynamic modeling of the Ba-Mg binary system, *Int. J. Mater. Res.*, 104 (2013) 358-363.

[76] D.F. Wu, L.Z. Ouyang, C. Wu, Q.F. Gu, H. Wang, J.W. Liu, M. Zhu, Phase transition and hydrogen storage properties of $\text{Mg}_{17}\text{Ba}_2$ compound, *J. Alloys Compd.*, 690 (2017) 519-522.

[77] P. Chiotti, R.W. Curtis, P.F. Woerner, Metal hydride reactions: II. Reaction of

hydrogen with CaMg_2 and CaCu_5 and thermodynamic properties of the compounds, *J. Less Common Met.*, 7 (1963) 120-126.

[78] D. Lupu, A. Biris, E. Indrea, R.V. Bucur, Effects of Ca additions on some Mg-alloy hydrides, *Int. J. Hydrogen Energy*, 8 (1983) 701-703.

[79] N. Terashita, E. Akiba, Hydrogenation properties of CaMg_2 based alloys, *Mater. Trans.*, 45 (2004) 2594-2597.

[80] M.L. Ma, R.M. Duan, L.Z. Ouyang, X.K. Zhu, Z.L. Chen, C.H. Peng, M. Zhu, Hydrogen storage and hydrogen generation properties of CaMg_2 -based alloys, *J. Alloys Compd.*, 691 (2017) 929-935.

[81] A.A. Nayeib-Hashemi, J.B. Clark, The Ga-Mg (Gallium-Magnesium) System, *Bulletin of Alloy Phase Diagrams* 6(1985) 434-439.

[82] D.F. Wu, L.Z. Ouyang, C. Wu, H. Wang, J.W. Liu, L.X. Sun, M. Zhu, Phase transition and hydrogen storage properties of Mg-Ga alloy, *J. Alloys Compd.*, 642 (2015) 180-184.

[83] G. Liang, R. Schulz, The reaction of hydrogen with Mg-Cd alloys prepared by mechanical alloying, *J. Mater. Sci.*, 39 (2004) 1557-1562.

[84] V.M. Skripnyuk, E. Rabkin, Mg_3Cd : A model alloy for studying the destabilization of magnesium hydride, *Int. J. Hydrogen Energy*, 37 (2012) 10724-10732.

[85] J.F. Zhang, Z.N. Li, Y.F. Wu, X.M. Guo, J.H. Ye, B.L. Yuan, S.M. Wang, L.J. Jiang, Recent advances on the thermal destabilization of Mg-based hydrogen storage materials, *RSC Adv.*, 9 (2019) 408-428.

[86] G. Liang, Synthesis and hydrogen storage properties of Mg-based alloys, *J. Alloys Compd.*, 370 (2004) 123-128.

[87] H.C. Zhong, H. Wang, J.W. Liu, D.L. Sun, M. Zhu, Altered desorption enthalpy of MgH_2 by the reversible formation of $\text{Mg}(\text{In})$ solid solution, *Scr. Mater.*, 65 (2011) 285-287.

[88] H. Wang, H.C. Zhong, L.Z. Ouyang, J.W. Liu, D.L. Sun, Q.G. Zhang, M. Zhu, Fully reversible de/hydriding of Mg base solid solutions with reduced reaction enthalpy and enhanced kinetics, *J. Phys. Chem. C*, 118 (2014) 12087-12096.

[89] F.P. Luo, H. Wang, L.Z. Ouyang, M.Q. Zeng, J.W. Liu, M. Zhu, Enhanced reversible hydrogen storage properties of a Mg-In-Y ternary solid solution, *Int. J. Hydrogen Energy*, 38 (2013) 10912-10918.

[90] Y.S. Lu, H. Wang, L.Z. Ouyang, J.W. Liu, M. Zhu, Reversible hydrogen storage and phase transformation with altered desorption pressure in $\text{Mg}_{90}\text{In}_5\text{Cd}_5$ ternary alloy, *J. Alloys Compd.*, 645 (2015) S103-S106.

[91] S. Zhang, A.F. Gross, S.L. Van Atta, M. Lopez, P. Liu, C.C. Ahn, J.J. Vajo, C.M. Jensen, The synthesis and hydrogen storage properties of a MgH_2 incorporated carbon aerogel scaffold, *Nanotechnology*, 20 (2009) 204027.

[92] Y. Liu, J. Zou, X. Zeng, X. Wu, H. Tian, W. Ding, J. Wang, A. Walter, Study on hydrogen storage properties of Mg nanoparticles confined in carbon aerogels, *Int. J. Hydrogen Energy*, 38 (2013) 5302-5308.

[93] Y.S. Au, M.K. Obbink, S. Srinivasan, P.C.M.M. Magusin, K.P. de Jong, P.E. de Jongh, The size dependence of hydrogen mobility and sorption kinetics for carbon-supported MgH_2 particles, *Adv. Funct. Mater.*, 24 (2014) 3604-3611.

[94] Y. Jia, C. Sun, L. Cheng, M. Abdul Wahab, J. Cui, J. Zou, M. Zhu, X. Yao, Destabilization of Mg-H bonding through nano-interfacial confinement by unsaturated carbon for hydrogen desorption from MgH_2 , *Phys. Chem. Chem. Phys.*, 15 (2013) 5814-5820.

1265 [95] H.J. Lin, W.H. Wang, M. Zhu, Room temperature gaseous hydrogen storage properties of Mg-
1266 based metallic glasses with ultrahigh Mg contents, *J. Non-Cryst. Solids*, 358 (2012) 1387-1390.

1267 [96] H.-J. Lin, C. Xu, M. Gao, Z. Ma, Y. Meng, L. Li, X. Hu, Y. Zhu, S. Pan, W. Li, Hydrogenation
1268 properties of five-component $Mg_{60}Ce_{10}Ni_{20}Cu_5X_5$ ($X = Co, Zn$) metallic glasses, *Intermetallics*, 108
1269 (2019) 94-99.

1270 [97] K.J. Gross, D. Chartouni, E. Leroy, A. Züttel, L. Schlapbach, Mechanically milled Mg composites
1271 for hydrogen storage: the relationship between morphology and kinetics, *J. Alloys Compd.*, 269 (1998)
1272 259-270.

1273 [98] H.J. Lin, C. Zhang, H. Wang, L.Z. Ouyang, Y.F. Zhu, L.Q. Li, W.H. Wang, M. Zhu, Controlling
1274 nanocrystallization and hydrogen storage property of Mg-based amorphous alloy via a gas-solid
1275 reaction, *J. Alloys Compd.*, 685 (2016) 272-277.

1276 [99] T. Spassov, U. Koster, Hydrogenation of amorphous and nanocrystalline Mg-based alloys, *J.*
1277 *Alloys Compd.*, 287 (1999) 243-250.

1278 [100] A. Zaluska, L. Zaluski, J.O. Strom-Olsen, Nanocrystalline magnesium for hydrogen storage, *J.*
1279 *Alloys Compd.*, 288 (1999) 217-225.

1280 [101] A. Zaluska, L. Zaluski, J.O. Strom-Olsen, Synergy of hydrogen sorption in ball-milled hydrides
1281 of Mg and Mg_2Ni , *J. Alloys Compd.*, 289 (1999) 197-206.

1282 [102] R. Schulz, J. Huot, G. Liang, S. Boily, G. Lalande, M.C. Denis, J.P. Dodelet, Recent
1283 developments in the applications of nanocrystalline materials to hydrogen technologies, *Mater. Sci.*
1284 *Eng., A*, 267 (1999) 240-245.

1285 [103] S. Orimo, H. Fujii, K. Ikeda, Notable hydriding properties of a nanostructured composite
1286 material of the Mg_2Ni -H system synthesized by reactive mechanical grinding, *Acta Mater.*, 45 (1997)
1287 331-341.

1288 [104] S. Orimo, H. Fujii, Hydriding properties of the Mg_2Ni -H system synthesized by reactive
1289 mechanical grinding, *J. Alloys Compd.*, 232 (1996) 16-19.

1290 [105] M.Y. Song, H.R. Park, Pressure-composition isotherms in the Mg_2Ni - H_2 system, *J. Alloys*
1291 *Compd.*, 270 (1998) 164-167.

1292 [106] X.Q. Tran, S.D. McDonald, Q. Gu, T. Yamamoto, K. Shigematsu, K. Aso, E. Tanaka, S.
1293 Matsumura, K. Nogita, In-situ investigation of the hydrogen release mechanism in bulk Mg_2NiH_4 , *J.*
1294 *Power Sources*, 341 (2017) 130-138.

1295 [107] B. Décamps, J.M. Joubert, R. Cerny, A. Percheron-Guégan, TEM study of the dislocations
1296 generated by hydrogen absorption/desorption in $LaNi_5$ and derivatives, *J Alloy Compd*, 404-406
1297 (2005) 570-575.

1298 [108] K. Edalati, J. Matsuda, A. Yanagida, E. Akiba, Z. Horita, Activation of TiFe for hydrogen storage
1299 by plastic deformation using groove rolling and high-pressure torsion: Similarities and differences, *Int J*
1300 *Hydrogen Energ*, 39 (2014) 15589-15594.

1301 [109] K. Edalati, J. Matsuda, M. Arita, T. Daio, E. Akiba, Z. Horita, Mechanism of activation of TiFe
1302 intermetallics for hydrogen storage by severe plastic deformation using high-pressure torsion, *Appl*
1303 *Phys Lett*, 103 (2013) 14391.

1304 [110] M. Danaie, S.X. Tao, P. Kalisvaart, D. Mitlin, Analysis of deformation twins and the partially
1305 dehydrogenated microstructure in nanocrystalline magnesium hydride (MgH_2) powder, *Acta Mater.*, 58
1306 (2010) 3162-3172.

1307 [111] T. Schober, The magnesium-hydrogen system: transmission electron microscopy, *Metall. Trans.*
1308 *A*, 12 (1981) 951-957.

- [112] T. Hongo, K. Edalati, M. Arita, J. Matsuda, E. Akiba, Z. Horita, Significance of grain boundaries and stacking faults on hydrogen storage properties of Mg₂Ni intermetallics processed by high-pressure torsion, *Acta Materialia*, 92 (2015) 46-54.
- [113] G.F. de Lima, S. Garroni, M.D. Baró, S. Suriñach, C.S. Kiminami, W.J. Botta, M.M. Peres, A.M. Jorge Junior, 2Mg-Fe alloys processed by hot-extrusion: Influence of processing temperature and the presence of MgO and MgH₂ on hydrogenation sorption properties, *J. Alloys. Compd.*, 509 (2011) S460-S463.
- [114] J.-H. Kim, J.-H. Kim, K.-T. Hwang, Y.-M. Kang, Hydrogen storage in magnesium based-composite hydride through hydriding combustion synthesis, *Int. J. Hydrogen Energy*, 35 (2010) 9641-9645.
- [115] X.H. Shao, Q.Q. Jin, Y.T. Zhou, H.J. Yang, S.J. Zheng, B. Zhang, Q. Chen, X.L. Ma, Segregation of solute atoms along deformation-induced boundaries in an Mg-Zn-Y alloy containing long period stacking ordered phase, *Materialia*, 6 (2019) 100287.
- [116] X.Q. Tran, S.D. McDonald, Effect of trace Na additions on the hydrogen absorption kinetics of Mg₂Ni, *J. Mater. Res.*, 31 (2016).
- [117] Z. Yanghuan, Z. Guofang, Y. Tai, H. Zhonghui, G. Shihai, Q. Yan, Z. Dongliang, Electrochemical and Hydrogen Absorption/Desorption Properties of Nanocrystalline Mg₂Ni-type Alloys Prepared by Melt Spinning, *Rare Metal Mat Eng*, 41 (2012) 2069-2074.
- [118] Y.-h. Zhang, B.-w. Li, H.-p. Ren, Z.-h. Ma, S.-h. Guo, X.-l. Wang, An electrochemical investigation of melt-spun nanocrystalline Mg₂₀Ni_{10-x}Cu_x (x = 0-4) electrode alloys, *Int. J. Hydrogen Energy*, 35 (2010) 2385-2392.
- [119] D. Kyoï, T. Sato, E. Rönnebro, N. Kitamura, A. Ueda, M. Ito, S. Katsuyama, S. Hara, D. Noréus, T. Sakai, A new ternary magnesium-titanium hydride Mg₇TiH_x with hydrogen desorption properties better than both binary magnesium and titanium hydrides, *J. Alloys Compd.*, 372 (2004) 213-217.
- [120] D. Moser, D.J. Bull, T. Sato, Structure and stability of high pressure synthesized Mg-TM hydrides (TM = Ti, Zr, Hf, V, Nb and Ta) as possible new hydrogen rich hydrides for hydrogen storage, *J. Mater. Chem. A*, 19 (2009) 8150-8161.
- [121] M. Calizzi, F. Venturi, M. Ponthieu, F. Cuevas, V. Morandi, T. Perkisas, S. Bals, L. Pasquini, Gas-phase synthesis of Mg-Ti nanoparticles for solid-state hydrogen storage, *Phys. Chem. Chem. Phys.*, 18 (2016) 141-148.
- [122] J.A. Puzskiel, P.A. Larochette, F.C. Gennari, Hydrogen storage properties of Mg_xFe (x = 2, 3 and 15) compounds produced by reactive ball milling, *J. Power Sources*, 186 (2009) 185-193.
- [123] B. Li, J.D. Li, H.J. Zhao, X.Q. Yu, H.Y. Shao, Mg-based metastable nano alloys for hydrogen storage, *Int. J. Hydrogen Energy*, 44 (2019) 6007-6018.
- [124] H.Y. Shao, K. Asano, H. Enoki, E. Akiba, Fabrication, hydrogen storage properties and mechanistic study of nanostructured Mg₅₀Co₅₀ body-centered cubic alloy, *Scr. Mater.*, 60 (2009) 818-821.
- [125] H.Y. Shao, J. Matsuda, H.W. Li, E. Akiba, A. Jain, T. Ichikawa, Y. Kojima, Phase and morphology evolution study of ball milled Mg-Co hydrogen storage alloys, *Int. J. Hydrogen Energy*, 38 (2013) 7070-7076.
- [126] N. Hanada, T. Ichikawa, H. Fujii, Catalytic effect of nanoparticle 3D-transition metals on hydrogen storage properties in magnesium hydride MgH₂ prepared by mechanical milling, *J. Phys. Chem. B*, 109 (2005) 7188-7194.

1353 [127] J. Dufour, J. Huot, Rapid activation, enhanced hydrogen sorption kinetics and air resistance in
1354 laminated Mg-Pd 2.5 at%, J. Alloys. Compd., (2007) L5-L7.

1355 [128] A.Y. Yermakov, N.V. Mushnikov, M.A. Uimin, V.S. Gaviko, A.P. Tankeev, A.V. Skripov,
1356 Hydrogen reaction kinetics of Mg-based alloys synthesized by mechanical milling, J. Alloys. Compd.,
1357 425 (2006) 367-372.

1358 [129] J. Cui, H. Wang, J.W. Liu, L.Z. Ouyang, Q.G. Zhang, D.L. Sun, X.D. Yao, M. Zhu, Remarkable
1359 enhancement in dehydrogenation of MgH_2 by a nano-coating of multi-valence Ti-based catalysts, J.
1360 Mater. Chem. A, 1 (2013).

1361 [130] J. Cui, J. Liu, H. Wang, L. Ouyang, D. Sun, M. Zhu, X. Yao, Mg-TM (TM: Ti, Nb, V, Co, Mo or
1362 Ni) core-shell like nanostructures: synthesis, hydrogen storage performance and catalytic mechanism,
1363 J. Mater. Chem. A, 2 (2014) 9645-9655.

1364 [131] W. Oelerich, T. Klassen, R. Bormann, Metal oxides as catalysts for improved hydrogen sorption
1365 in nanocrystalline Mg-based materials, J. Alloys Compd., 315 (2001) 237-242.

1366 [132] Y. Makihara, K. Umeda, F. Shoji, K. Kato, Y. Miyairi, Cooperative dehydriding mechanism in a
1367 mechanically milled Mg-50 mass% ZrMn_2 composite, J. Alloys. Compd., 455 (2008) 385-391.

1368 [133] C.X. Shang, Z.X. Guo, Effect of carbon on hydrogen desorption and absorption of mechanically
1369 milled MgH_2 , J. Power Sources, 129 (2004) 73-80.

1370 [134] A. Takasaki, Y. Furuya, M. Katayama, Mechanical alloying of graphite and magnesium powders,
1371 and their hydrogenation, J. Alloys. Compd., 446 (2007) 110-113.

1372 [135] A. Patah, A. Takasaki, J.S. Szmyd, Influence of multiple oxide ($\text{Cr}_2\text{O}_3/\text{Nb}_2\text{O}_5$) addition on the
1373 sorption kinetics of MgH_2 , Int. J. Hydrogen Energy, 34 (2009) 3032-3037.

1374 [136] A. Ranjbar, Z.P. Guo, X.B. Yu, D. Attard, A. Calka, H.K. Liu, Effects of SiC nanoparticles with
1375 and without Ni on the hydrogen storage properties of MgH_2 , Int. J. Hydrogen Energy, 34 (2009) 7263-
1376 7268.

1377 [137] K.F. Aguey Zinsou, J.R. Ares Fernandez, T. Klassen, R. Bormann, Effect of Nb_2O_5 on MgH_2
1378 properties during mechanical milling, Int. J. Hydrogen Energy, 32 (2007) 2400-2407.

1379 [138] O. Friedrichs, F. Agueyzinsou, J. Fernandez, J. Sanchezlopez, A. Justo, T. Klassen, R. Bormann,
1380 A. Fernandez, MgH_2 with Nb_2O_5 as additive, for hydrogen storage: Chemical, structural and kinetic
1381 behavior with heating, Acta Materialia, 54 (2006) 105-110.

1382 [139] G. Liang, J. Huot, S. Boily, A. Van Neste, R. Schulz, Catalytic effect of transition metals on
1383 hydrogen sorption in nanocrystalline ball milled MgH_2 -Tm (Tm = Ti, V, Mn, Fe and Ni) systems, J.
1384 Alloys. Compd., 292 (1999) 247-252.

1385 [140] D.L. Narayanan, A.D. Lueking, Mechanically milled coal and magnesium composites for
1386 hydrogen storage, Carbon, 45 (2007) 805-820.

1387 [141] M. Khrussanova, M. Terzieva, P. Peshev, E. Ivanov, On the hydriding and dehydriding kinetics of
1388 magnesium with a titanium dioxide admixture, Mater. Res. Bull. , 22 (1987) 405-412.

1389 [142] M. Khrussanova, M. Terzieva, P. Peshev, I. Konstanchuk, E. Ivanov, Hydriding of mechanically
1390 alloyed mixtures of magnesium with MnO_2 , Fe_2O_3 and NiO, Mater. Res. Bull. , 26 (1991) 561-567.

1391 [143] V.V. Bhat, A. Rougier, L. Aymard, G.A. Nazri, J.M. Tarascon, High surface area niobium oxides
1392 as catalysts for improved hydrogen sorption properties of ball milled MgH_2 , J. Alloys. Compd., 460
1393 (2008) 507-512.

1394 [144] N. Bazzanella, R. Checchetto, A. Miotello, C. Sada, P. Mazzoldi, P. Mengucci, Hydrogen kinetics
1395 in magnesium hydride: On different catalytic effects of niobium, Appl Phys Lett, 89 (2006) 014101.

1396 [145] G. Barkhordarian, T. Klassen, R. Bormann, Fast hydrogen sorption kinetics of nanocrystalline

1397 Mg using Nb₂O₅ as catalyst, *Scr. Mater.*, 49 (2003) 213-217.

1398 [146] V.V. Bhat, A. Rougier, L. Aymard, X. Darok, G.A. Nazri, J.M. Tarascon, Catalytic activity of
1399 oxides and halides on hydrogen storage of MgH₂, *J. Power Sources*, 159 (2006) 107-110.

1400 [147] S.N. Klyamkin, Metal hydride compositions on the basis of magnesium as materials for hydrogen
1401 accumulation, *Russian Journal of General Chemistry*, 77 (2007) 712-720.

1402 [148] E.D. Wang, Z.X. Yu, Z.Y. Liu, Hydrogen storage properties of nanocomposite Mg-Ni-MnO₂
1403 made by mechanical milling, *Trans. Nonferrous Met. Soc. China*, 12 (2002) 227.

1404 [149] J.X. Zou, H. Guo, X.Q. Zeng, S. Zhou, X. Chen, W.J. Ding, Hydrogen storage properties of Mg-
1405 TM-La (TM = Ti, Fe, Ni) ternary composite powders prepared through arc plasma method, *Int. J.*
1406 *Hydrogen Energy*, 38 (2013) 8852-8862.

1407 [150] I.E. Malka, T. Czujko, J. Bystrzycki, Catalytic effect of halide additives ball milled with
1408 magnesium hydride, *Int. J. Hydrogen Energy*, 35 (2010) 1706-1712.

1409 [151] E. Ivanov, I. Konstanchuk, B. Bokhonov, V. Boldyrev, Hydrogen interaction with mechanically
1410 alloyed magnesium-salt composite materials, *J. Alloys Compd.*, 359 (2003) 320-325.

1411 [152] M. Ismail, Effect of LaCl₃ addition on the hydrogen storage properties of MgH₂, *Energy*, 79
1412 (2015) 177-182.

1413 [153] D.P. Broom, *Hydrogen storage materials: the characterization of their storage properties.*,
1414 Springer Science & Business Media, 2011.

1415 [154] L.B. Wang, Y.J. Wang, H.T. Yuan, Development of Mg-based hydrogen storage alloy, *J. Mater.*
1416 *Sci. Technol.*, 17 (2001) 590-596.

1417 [155] M. Zhu, Y. Gao, X.Z. Che, Y.Q. Yang, C.Y. Chung, Hydriding kinetics of nano-phase composite
1418 hydrogen storage alloys prepared by mechanical alloying of Mg and MmNi_{5-x}(CoAlMn)_x, *J. Alloys*
1419 *Compd.*, 330-332 (2002) 708-713.

1420 [156] J. Liu, X. Zhang, Q. Li, K.C. Chou, K.D. Xu, Investigation on kinetics mechanism of hydrogen
1421 absorption in the La₂Mg₁₇-based composites, *Int. J. Hydrogen Energy*, 34 (2009) 1951-1957.

1422 [157] C.H. Peng, M. Zhu, Microstructure and hydrogen storage properties of a multi-phase
1423 Ml_{0.7}Mg_{0.3}Ni_{3.2} hydrogen storage alloy, *J. Alloys Compd.*, 375 (2004) 324-329.

1424 [158] M. Zhu, C.H. Peng, L.Z. Ouyang, Y.Q. Tong, The effect of nanocrystalline formation on the
1425 hydrogen storage properties of AB₃-base Ml-Mg-Ni multi-phase alloys, *J. Alloys Compd.*, 426 (2006)
1426 316-321.

1427 [159] H. Wang, H.J. Lin, W.T. Cai, L.Z. Ouyang, M. Zhu, Tuning kinetics and thermodynamics of
1428 hydrogen storage in light metal element based systems-a review of recent progress, *J. Alloys Compd.*,
1429 658 (2016) 280-300.

1430 [160] J.J. Vajo, T.T. Salguero, A.F. Gross, S.L. Skeith, G.L. Olson, Thermodynamic destabilization and
1431 reaction kinetics in light metal hydride systems, *J. Alloys Compd.*, 446-447 (2007) 409-414.

1432 [161] J.J. Vajo, F. Mertens, C.C. Ahn, J. R. C. Bowman, B. Fultz, Altering Hydrogen Storage Properties
1433 by Hydride Destabilization through Alloy Formation: LiH and MgH₂ Destabilized with Si, *J. Phys.*
1434 *Chem. B*, 108 (2004) 13977-13983.

1435 [162] A.L. Chaudhary, D.A. Sheppard, M. Paskevicius, C.J. Webb, E.M. Gray, C.E. Buckley, Mg₂Si
1436 nanoparticle synthesis for high pressure hydrogenation, *J. Phys. Chem. C*, 118 (2014) 1240-1247.

1437 [163] S.T. Kelly, S.L. Van Atta, J.J. Vajo, G.L. Olson, B.M. Clemens, Kinetic limitations of the Mg₂Si
1438 system for reversible hydrogen storage, *Nanotechnology*, 20 (2009) 204017.

1439 [164] F.C. Gennari, F.J. Castro, G. Urretavizcaya, G. Meyer, Catalytic effect of Ge on hydrogen
1440 desorption from MgH₂, *J. Alloys Compd.*, 334 (2002) 277-284.

1441 [165] G.S. Walker, M. Abbas, D.M. Grant, C. Udeh, Destabilisation of magnesium hydride by
 1442 germanium as a new potential multicomponent hydrogen storage system, *Chem. Commun.*, 47 (2011).
 1443 [166] H.C. Zhong, H. Wang, L.Z. Ouyang, M. Zhu, Microstructure and hydrogen storage properties of
 1444 Mg-Sn nanocomposite by mechanical milling, *J. Alloys Compd.*, 509 (2011) 4268-4272.
 1445 [167] G. Urretavizcaya, G.O. Meye, Metastable hexagonal Mg₂Sn obtained by mechanical alloying, *J.*
 1446 *Alloys Compd.*, 339 (2002) 211-215.
 1447 [168] K. Nogita, S. Ockert, J. Pierce, M.C. Greaves, C.M. Goulay, A.K. Dahle, Engineering the Mg-
 1448 Mg₂Ni eutectic transformation to produce improved hydrogen storage alloys, *Int. J. Hydrogen Energy*,
 1449 34 (2009) 7686-7691.
 1450 [169] S. Bouaricha, J.P. Dodelet, D. Guay, Hydriding behavior of Mg-Al and leached Mg-Al
 1451 compounds prepared by high-energy ball-milling., *J. Alloys Compd.*, 297 (2000) 282-293.
 1452 [170] J.C. Crivello, T. Nobuki, T. Kuji, Improvement of Mg-Al alloys for hydrogen storage
 1453 applications, *Int. J. Hydrogen Energy*, 34 (2009) 1937-1943.
 1454 [171] W.P. Kalisvaart, C.T. Harrower, J. Haagsma, B. Zahiri, E.J. Lubber, C. Ophus, E. Poirier, H.
 1455 Fritzsche, D. Mitlin, Hydrogen storage in binary and ternary Mg-based alloys: A comprehensive
 1456 experimental study, *Int. J. Hydrogen Energy*, 35 (2010) 2091-2103.
 1457 [172] C.S. Zhou, Z.Z. Fang, C. Ren, J.Z. Li, J. Lu, Effect of Ti intermetallic catalysts on hydrogen
 1458 storage properties of magnesium hydride, *J. Phys. Chem. C*, 117 (2013) 12973-12980.
 1459 [173] C. Zhou, Z.Z. Fang, J. Lu, X. Zhang, Thermodynamic and kinetic destabilization of magnesium
 1460 hydride using Mg-In solid solution alloys, *J. Am. Chem. Soc.*, 135 (2013) 10982-10985.
 1461 [174] L.Z. Ouyang, Z.J. Cao, H. Wang, J.W. Liu, D.L. Sun, Q.A. Zhang, M. Zhu, Enhanced
 1462 dehydriding thermodynamics and kinetics in Mg(In)-MgF₂ composite directly synthesized by plasma
 1463 milling, *J. Alloys Compd.*, 586 (2014) 113-117.
 1464 [175] Z.J. Cao, L.Z. Ouyang, Y.Y. Wu, H. Wang, J.W. Liu, F. Fang, D.L. Sun, Q.G. Zhang, M. Zhu,
 1465 Dual-tuning effects of In, Al, and Ti on the thermodynamics and kinetics of Mg₈₅In₅Al₅Ti₅ alloy
 1466 synthesized by plasma milling, *J. Alloys Compd.*, 623 (2015) 354-358.
 1467 [176] Y.S. Lu, M. Zhu, H. Wang, Z.M. Li, L.Z. Ouyang, J.W. Liu, Reversible de-/hydriding
 1468 characteristics of a novel Mg₁₈In₁Ni₃ alloy, *Int. J. Hydrogen Energy*, 39 (2014) 14033-14038.
 1469 [177] Y.S. Lu, H. Wang, J.W. Liu, L.Z. Ouyang, L.K. Zhu, D.L. Zhang, M. Zhu, Reversible
 1470 de-/hydriding reactions between two new Mg-In-Ni compounds with improved thermodynamics and
 1471 kinetics, *J. Phys. Chem. C*, 119 (2015) 26858-26865.
 1472 [178] C. Suryanarayana, Mechanical alloying and milling, *Prog. Mater. Sci.*, 46 (2001) 1-184.
 1473 [179] A. Baldi, B. Dam, Thin film metal hydrides for hydrogen storage applications, *J. Mater. Chem.*,
 1474 21 (2011) 4021-4026.
 1475 [180] C.E. Buckley, H.K. Birnbaum, J.S. Lin, S. Spooner, D. Bellmann, P. Staron, T.J. Udovic, E.
 1476 Hollar, Characterization of H defects in the aluminium± hydrogen system using small-angle scattering
 1477 techniques, *J. Appl. Cryst.*, 34 (2001) 119-129.
 1478 [181] Y. Zhang, T. Yang, Y. Cai, Z. Hou, H. Ren, D. Zhao, Electrochemical hydrogen storage
 1479 characteristics of La_{0.75-x}M_xMg_{0.25}Ni_{3.2}Co_{0.2}Al_{0.1} (M = Zr, Pr; x = 0, 0.1) alloys prepared by melt
 1480 spinning, *Rare Metals*, 31 (2012) 457-465.
 1481 [182] V.M. Skripnyuk, E. Rabkin, Y. Estrin, R. Lapovok, The effect of ball milling and equal channel
 1482 angular pressing on the hydrogen absorption/desorption properties of Mg-4.95 wt% Zn-0.71 wt% Zr
 1483 (ZK60) alloy, *Acta Materialia*, 52 (2004) 405-414.
 1484 [183] D.R. Leiva, J.A.M. Jorge, T.T. Ishikawa, W.J. Botta, Hydrogen Storage in Mg and Mg-Based

Alloys and Composites Processed by Severe Plastic Deformation, *Materials Transactions*, 60 (2019) 1561-1570.

[184] C. G., *Nanostructures and nanomaterials properties and applications*, World Scientific, New Jersey, 2004.

[185] I. Haas, A. Gedanken, Synthesis of metallic magnesium nanoparticles by sonoelectrochemistry, *Chem. Commun.*, (2008) 1795-1797.

[186] A.A. Cesario Asselli, N. Bourbeau Hébert, J. Huot, The role of morphology and severe plastic deformation on the hydrogen storage properties of magnesium, *Int. J. Hydrogen Energy*, 39 (2014) 12778-12783.

[187] K. Edalati, H. Emami, Y. Ikeda, H. Iwaoka, I. Tanaka, E. Akiba, Z. Horita, New nanostructured phases with reversible hydrogen storage capability in immiscible magnesium-zirconium system produced by high-pressure torsion, *Acta Materialia*, 108 (2016) 293-303.

[188] R.Z. Valiev, T.G. Langdon, Principles of equal-channel angular pressing as a processing tool for grain refinement, *Progress in Materials Science*, 51 (2006) 881-981.

[189] M. Faisal, A. Gupta, S. Shervani, K. Balani, A. Subramaniam, Enhanced hydrogen storage in accumulative roll bonded Mg-based hybrid, *Int. J. Hydrogen Energy*, 40 (2015) 11498-11505.

[190] M. Danaie, C. Mauer, D. Mitlin, J. Huot, Hydrogen storage in bulk Mg-Ti and Mg-stainless steel multilayer composites synthesized via accumulative roll-bonding (ARB), *Int. J. Hydrogen Energy*, 36 (2011) 3022-3036.

[191] S. Løken, J.K. Solberg, J.P. Maehlen, R.V. Denys, M.V. Lototsky, B.P. Tarasov, V.A. Yartys, Nanostructured Mg-Mn-Ni hydrogen storage alloy: Structure-properties relationship, *J. Alloys. Compd.*, 446-447 (2007) 114-120.

[192] V. Skripnyuk, E. Buchman, E. Rabkin, Y. Estrin, M. Popov, S. Jorgensen, The effect of equal channel angular pressing on hydrogen storage properties of a eutectic Mg-Ni alloy, *J. Alloys. Compd.*, 436 (2007) 99-106.

[193] J. Dufour, J. Huot, Rapid activation, enhanced hydrogen sorption kinetics and air resistance in laminated Mg-Pd 2.5 at.%, *J. Alloys. Compd.*, 439 (2007) L5-L7.

[194] N. Takeichi, K. Tanaka, H. Tanaka, T.T. Ueda, Y. Kamiya, M. Tsukahara, H. Miyamura, S. Kikuchi, Hydrogen storage properties of Mg/Cu and Mg/Pd laminate composites and metallographic structure, *J. Alloys. Compd.*, 446-447 (2007) 543-548.

[195] T.T. Ueda, M. Tsukahara, Y. Kamiya, S. Kikuchi, Preparation and hydrogen storage properties of Mg-Ni-Mg₂Ni laminate composites, *J. Alloys. Compd.*, 386 (2005) 253-257.

[196] K. Suganuma, H. Miyamura, S. Kikuchi, N. Takeichi, K. Tanaka, H. Tanaka, N. Kuriyama, T.T. Ueda, M. Tsukahara, Hydrogen Storage Properties of Mg-Al Alloy Prepared by Super Lamination Technique, *Advanced Materials Research*, 26-28 (2007) 857-860.

[197] A.A.C. Asselli, D.R. Leiva, J. Huot, M. Kawasaki, T.G. Langdon, W.J. Botta, Effects of equal-channel angular pressing and accumulative roll-bonding on hydrogen storage properties of a commercial ZK60 magnesium alloy, *Int. J. Hydrogen Energy*, 40 (2015) 16971-16976.

[198] D.R. Leiva, D. Fruchart, M. Bacia, G. Girard, N. Skryabina, A.C.S. Villela, S. Miraglia, D.S. Santos, W.J. Botta, Mg alloy for hydrogen storage processed by SPD, *Int. J. Mat. Res.*, 100 (2009) 1739-1746.

[199] J. Huot, N.Y. Skryabina, D. Fruchart, Application of Severe Plastic Deformation Techniques to Magnesium for Enhanced Hydrogen Sorption Properties, *Metals*, 2 (2012) 329-343.

[200] W.J. Botta, A.M. Jorge, M. Veron, E.F. Rauch, E. Ferrie, A.R. Yavari, J. Huot, D.R. Leiva, H-

sorption properties and structural evolution of Mg processed by severe plastic deformation, *J. Alloys. Compd.*, 580 (2013) S187-S191.

[201] M. Au, Hydrogen storage properties of magnesium based nanostructured composite materials, *Mater. Sci. Eng., B*, 117 (2005) 37-44.

[202] S. Kalinichenka, L. Rontzsch, T. Riedl, T. Weissgarber, B. Kieback, Hydrogen storage properties and microstructure of melt-spun $Mg_{90}Ni_8RE_2$ ($RE = Y, Nd, Gd$), *Int. J. Hydrogen Energy*, 36 (2011) 10808-10815.

[203] E.S. Cho, A.M. Ruminski, Y.S. Liu, P.T. Shea, S. Kang, E.W. Zaia, J.Y. Park, Y.D. Chuang, J.M. Yuk, X.W. Zhou, T.W. Heo, J.H. Guo, B.C. Wood, J.J. Urban, Hierarchically controlled inside-out doping of Mg nanocomposites for moderate temperature hydrogen storage, *Adv. Funct. Mater.*, 27 (2017).

[204] G.S. Walker, D.M. Grant, T.C. Price, X.B. Yu, V. Legrand, High capacity multicomponent hydrogen storage materials: Investigation of the effect of stoichiometry and decomposition conditions on the cycling behaviour of $LiBH_4$ - MgH_2 , *J. Power Sources*, 194 (2009) 1128-1134.

[205] W. Liu, E.J. Setijadi, K.F. Aguey-Zinsou, Tuning the thermodynamic properties of MgH_2 at the nanoscale via a catalyst or destabilizing element coating strategy, *J. Phys. Chem. C*, 118 (2014) 27781-27792.

[206] C. Lu, J.X. Zou, X.Q. Zeng, W.J. Ding, Hydrogen storage properties of core-shell structured $Mg@TM$ ($TM = Co, V$) composites, *Int. J. Hydrogen Energy*, 42 (2017) 15246-15255.

[207] Q.Y. Zhang, Y. Wang, L. Zang, X.Y. Chang, L.F. Jiao, H.T. Yuan, Y.J. Wang, Core-shell $Ni_3N@$ Nitrogen-doped carbon: synthesis and application in MgH_2 , *J. Alloys Compd.*, 703 (2017) 381-388.